

COMPUTER STOCHASTICS IN SCALAR QUANTUM FIELD THEORY*

C.B. LANG
Inst. f. theoret. Physik
Universität Graz
Universitätsplatz 5
A-8010 Graz, AUSTRIA

Abstract. This is a series of lectures on Monte Carlo results on the non-perturbative, lattice formulation approach to quantum field theory. Emphasis is put on 4D scalar quantum field theory. I discuss real space renormalization group, fixed point properties and logarithmic corrections, partition function zeroes, the triviality bound on the Higgs mass, finite size effects, Goldstone bosons and chiral perturbation theory, and the determination of scattering phase shifts for some scalar models.

Key words: Scalar quantum field theory, Φ^4 model, Monte Carlo methods

1. LATTICE QUANTUM FIELD THEORY

In this series of lectures I attempt to cover some numerical applications to stochastic analysis in relativistic quantum field theory (QFT). Following a more general introduction I then focus on the non-perturbative quantization of *scalar* QFT. This emphasis is dictated by the limited time and place available as well as by the progress in the subject. Scalar QFT meanwhile is the most advanced of the interesting models, both in theoretical understanding as well as in numerical stochastic calculations.

If you are interested in particular topics of lattice field (including gauge field) theory, a good starting point is to look up the proceedings of the annual workshops in lattice field theory. For the recent years they have been published in Nucl. Phys. B (Proc. Suppl.); up to now there are volumes 9(1989), 17(1990), 20(1991), 26(1992), 30(1993). In every one of these volumes there are also reviews, although mainly targeted at the devotees of the field.

There are only few books giving surveys. Almost all important results of the first, hot days of Monte Carlo computations are given in the reprint collection [116] and the monograph [24]. The more rigorously oriented person should maybe start with [120]. Recently two volumes on the field have been published, one is the monograph [118] and the other contains a collection of review article written by experts on various subtopics [25].

In the first part I attempt an overview on lattice field theory and the related computational issues. The role of the Φ^4 model in particle physics is discussed and the lattice formulation for that model is introduced. In the second chapter some rigorous statements on the model are reviewed and then lattice calculation results concerning the fixed point structure and the issue of triviality are presented. In the

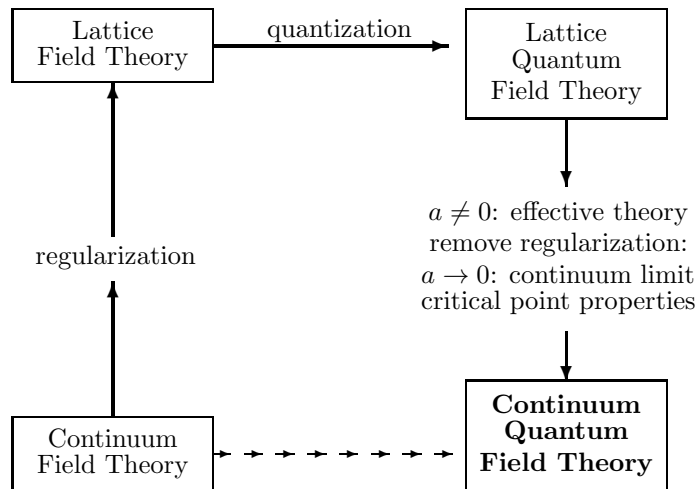
* to appear in *Stochastic Analysis and Applications in Physics*, Proc. of the NATO ASI in Funchal, Madeira, Aug. 1993, ed. L. Streit (Kluwer Acad. Publishers, Dordrecht: 1994)

subsequent chapter further results on the so-called triviality bound are discussed; also the particle spectrum and in particular the finite size effects produced by the massless Goldstone states are reviewed. In the last section I present recent results that use the scalar model as a testing ground for new methods to determine scattering phase shifts non-perturbatively.

1.1. Regularization and Quantization

1.1.1. Space-time Lattice

Quantum field theory usually is discussed within the perturbative framework. Even there it is obvious that there are divergences in elementary contributions. In a functional integration (Feynman path integral) formulation one finds that the integration is not well-defined. The functional integral has to be regularized in order to be able to identify the singularities.



Replacing the space-time continuum by a lattice provides a suitable regularization as well as a computational tool [142]. We can define the continuum QFT as the limit of the lattice QFT for vanishing lattice spacings. Important symmetries of the Lagrangian (like e.g. gauge invariance) may be sustained in the lattice formulation. On the other hand, obvious symmetries of space-time like translational and rotational invariance are replaced by their lattice subgroups and eventual recovery in the continuum limit has to be established.

We will discuss euclidean QFT. The regularization replaces the continuous, $O(4)$ symmetric space-time arena by a (in practical calculations) finite lattice with symmetry $O(4; \mathbb{Z})$.

lattice	Λ e.g. $\mathbb{Z}_N^D \subset \mathbb{Z}^D$
field	$\Phi : \Lambda \mapsto \mathbb{X}$ (e.g. \mathbb{C}) $\in \Gamma$
configuration	$\Gamma \in \mathbb{X}^\Lambda$
action	$S_\Lambda : \Gamma \mapsto \mathbb{R}$
partition function	$Z_\Lambda = \int d\mu_\Lambda(\Phi) \exp[S_\Lambda(g, \Phi)]$
free energy	$F_\Lambda = \ln Z_\Lambda$
Gibbs factor	$\rho_\Lambda(\Phi) = Z_\Lambda^{-1} \exp[S_\Lambda(g, \Phi)]$
expectation values	$\langle A \rangle_\Lambda = \int d\mu_\Lambda(\Phi) \rho_\Lambda(\Phi) A(\Phi)$

Quantization thus amounts to determination of expectation values in a 4D statistical system, like e.g. the Ising model (cf. for instance [117]). With g we denote the coupling constant (or a vector of constants) parametrizing the action.

1.1.2. Scaling

The focus of interest in that process are two limits:

Thermodynamic limit: The infinite volume limit $|\Lambda| \rightarrow \infty$.

Continuum limit: Is obtained at a critical point $g \rightarrow g_c$ in coupling constant space, where the lattice spacing constant $a(g) \rightarrow 0$; the lattice spacing acts as a regularization parameter.

The second limit needs some discussion. The physical quantities like mass or length of the continuum theory should approach constant values, however on the lattice they are expressed in multiples of the lattice spacing a . These lattice quantities are dimensionless and are determined from the connected correlation functions (propagators) of some operators

$$\begin{aligned} \langle A(0)A(x) \rangle_c &\propto \exp(-x/\xi) = \exp(-ax/a\xi) \\ &= \exp(-m_{\text{phys}}ax), \quad \text{i.e. } m_{\text{phys}}a = 1/\xi. \end{aligned} \quad (1.1)$$

These correlation functions describe propagation in euclidean time and the operators may be representing n-particle states. The exponential decay should hold for sensible theories [120].

Only at a critical point the correlation length ξ diverges¹ and allows to let $a \rightarrow 0$ while keeping a fixed value for the physical mass parameter. One has to fix the scale

¹ At the critical point the correlation function decay polynomially $\propto |x|^{d-2+\eta}$

$a(g)$ by trading one physical parameter. Once the scale is set, all other parameters may then be expressed in terms of this scale parameter $a(g)$. However, all other physical parameters should scale correspondingly, only then can we identify the correct continuum theory.

In practical situations we distinguish between two qualities of scaling behaviour.

Scaling: The dimensionless ratios like $\frac{m_1(g)a(g)}{m_2(g)a(g)} = \frac{m_1(g)}{m_2(g)}$ scale towards the physical ratio $\frac{m_1}{m_2}$ as $a \rightarrow 0$

Asymptotic scaling: The scaling behaviour $a(g) \propto f(g)$ as determined from the renormalization group β -function.

The relative importance of irrelevant operators determines the quality of scaling. Whereas scaling may be observed quite early one has to be quite close to the critical point in order to observe asymptotic scaling.

1.1.3. Continuum Limit

Let us collect some points important in the context of the continuum limit.

- The lattice action should obey Osterwalder-Seiler positivity when approaching the continuum limit in order to guarantee existence of a transfer matrix formalism and positive norm Hilbert states [115].
- The continuum limit is obtained at a critical point (2nd order phase transition) of the lattice system: $g \rightarrow g^*$, where the dimensionless correlation length $\xi \rightarrow \infty$.
- All physical quantities are multiples of the lattice spacing and should scale correspondingly, $a(g) \rightarrow 0$ for $g \rightarrow g^*$.
- Lattice translation invariance $\text{mod}(a)$ should become continuous translation invariance.
- The space-time symmetry (cubic group for cubic lattices) should become the continuous $O(4)$ (rotational) invariance. This may be observed in off-shell observables (like the 1-particle propagator) as well as in on-shell ones (like differential scattering cross-sections).
- Fields, couplings and masses in the lattice action are bare quantities and are renormalized in the quantization in continuum limit. Renormalized quantities will have a subscript r henceforth.
- Because of renormalization, the continuum properties of a quantized theory may be quite different from those of the bare theory. In statistical physics this observation is linked to the notion of universality: Theories with different micro-structure may show universal critical (macroscopic) properties. Since the critical properties are just the physical properties of our quantized continuum theory this limits the class of liable continuum QFTs.

All these points should be observed in a sensible investigation of the continuum limit. Most of these properties can be studied only in the quantized theory in a non-perturbative environment. In existing Monte Carlo calculations several of these features have been checked and some of these checks will be discussed in this series of lectures.

1.2. Particle Physics and the Φ^4 Model

1.2.1. Lattice Fields

Typically we have to deal with the following types of lattice fields.

Scalar bosons: Occur in the action usually with local terms like Φ_x , Φ_x^2 , Φ_x^4 and nearest neighbour terms like $\Phi_x U_{x,\mu} \Phi_{x+\mu}$; the n.n. term is a lattice discretization of the continuum derivative term. Monte Carlo integration methods for these fields include the standard Metropolis or heat bath updating as well as cluster- and multigrid methods. The computational effort grows with $O(L^4)$ up to $O(L^6)$ depending on the algorithm (L denotes the linear extension of the 4D lattice),

Gauge (vector) bosons: Action terms include the Wilson plaquette interaction $Tr U_p$, where the plaquette variable is the path ordered product of link fields $U_{x,\mu}$ around a plaquette. The gauge field coupling $\beta \propto \frac{1}{g^2}$ where g is the usual perturbative coupling constant. Monte Carlo updating algorithms include Metropolis, heat bath and overrelaxation; some progress has been made in designing multigrid algorithms. The computational effort grows with $O(L^5)$ up to $O(L^6)$.

Fermions: Occur in the action with terms like $\bar{\Psi}_x \Psi_x$ and $\bar{\Psi}_x Q_{xy} \Psi_y$ which includes Dirac γ -matrices and nearest neighbour coupling κ . Updating algorithms are an order of magnitude more demanding with regard to computational resources; they include molecular dynamics updating, Langevin and “hybrid” Monte Carlo methods as well as some recent attempts towards multigrid methods. The central numerical problem is the inversion of the lattice Dirac operator Q , thus the total effort grows with $O(L^9)$ up to $O(L^{16})$ depending on the algorithm.

For the formulation of the models on finite volumes one usually assumes periodic boundary conditions, $\Phi(x + L\hat{\mu}) = \Phi(x)$ (for fermions: antiperiodic b.c.). The implicit assumption is that the thermodynamic limit should be independent on the choice of boundary conditions. Periodic b.c. seem to produce relatively small finite size effects.

1.2.2. Scalar Model

The standard model of electroweak and strong interactions describes extremely successfully nowadays results in particles physics in an energy domain from a few MeV up to more than 100 GeV. Its central symmetry is $SU(2) \times U(1) \times SU(3)$. The $SU(3)$ is that of QCD, represented by quarks, gluons and their interaction. The non-perturbative lattice study of that model is a central topic in lattice calculations [29], but I will not try to cover it here. The symmetry groups $SU(2) \times U(1)$ are those of quantum flavour dynamics and are represented by the fundamental leptons, 4 gauge bosons and the doublet $\Phi = (\Phi_1 + i\Phi_2, \Phi_3 + i\Phi_4)$ of complex Higgs fields. In particular the action for the Higgs fields has a symmetry $SU(2)_L \times SU(2)_R$ isomorphic to $O(4)$. Thus we may represent the Higgs fields by a vector of 4 real scalar fields, too.

Fig. 1. Standard model symmetry breaking scenario.

In the standard scenario one assumes that there is a symmetry breaking potential like the well-known Mexican hat potential $\lambda(\Phi^2 - 1)^2$. In the Goldstone realization the vacuum chooses spontaneously one direction (out of the infinite set of inequivalent representations, cf. fig. 1), thus one is left with one massive component (the Higgs particle) and three massless components (the Goldstone modes), which, in the so-called Higgs mechanism, become the longitudinal modes of three of the (originally massless) vector bosons. The three vector bosons acquire mass in that process. For sake of the later discussion let us distinguish the two processes:

Symmetry breaking: The $O(4)$ symmetry is spontaneously broken and in the new vacuum we find one massive and three massless modes.

Mass generation: Three massless gauge bosons buddy with the three Goldstone modes and become massive gauge bosons, Z and W^\pm .

Both mechanisms are non-perturbative as they involve infinitely many degrees of freedom. The results mentioned are based on tree-level perturbation theory and some additional assumption about the vacuum structure. One of the basic questions to be answered in the non-perturbative lattice simulations is, whether these results survive quantization and whether they remain valid at arbitrary Higgs coupling strength.

The essential non-perturbative ingredient is the $O(4)$ Φ^4 model. This is the main motivation for studying that theory non-perturbatively in some detail.

1.2.3. The Φ^4 Model

The continuum action

$$S_{cont} = \int dx \left[\frac{1}{2} (\partial_\mu \Phi_x)^2 + \frac{1}{2} m_{cont}^2 \Phi_x^2 + \frac{1}{4!} \lambda_{cont} (\Phi_x^2)^2 + j_{cont} \Phi_x \right] \quad (1.2)$$

has three parameters, the bare mass, the 4-point coupling, and the external field. Discretization is not unique and a particular simple form of a lattice action is obtained by replacing the derivative term by a nearest neighbour difference. With

suitable redefinitions of the couplings we get

$$S_{latt} = \sum_{\Lambda} \left[-2\kappa \sum_{\mu} \Phi_x \Phi_{x+\mu} + \lambda (\Phi_x^2 - 1)^2 + J\Phi_x \right]. \quad (1.3)$$

We have several important cases.

- $\Phi_x \in \mathbb{Z}_2$: the Ising model,
- $\Phi_x \in \mathbb{R}$: the simple 1-component Φ^4 model,
- $\Phi_x \equiv \Phi_x^\alpha \in O(4)$: the 4-component Φ^4 model, i.e. the Higgs model.

For notational simplicity we sometimes use field variables

$$\varphi \equiv \sqrt{2\kappa}\Phi, \quad j \equiv J/\sqrt{2\kappa}. \quad (1.4)$$

In the form (1.3) we identify immediately two limits of the system. For $\lambda \rightarrow 0$ we approach a gaussian model. For $\lambda \rightarrow \infty$ only configurations with $|\Phi_x| = 1$ contribute and we have a nonlinear sigma model (for the 1-component version: Ising model). The coupling κ , λ and j in the lattice action are bare quantities, given at the generic lattice scale a . Values measured in the quantized system like e.g. the mass or the 4-point coupling are renormalized quantities and will be denoted by a subscript: m_r, λ_r .

At the critical point of the model, $\kappa = \kappa_c$, critical exponents characterize the singular behaviour of various quantities [125, 104]. Introducing the reduced coupling

$$t \equiv \frac{\kappa_c - \kappa}{\kappa_c} \quad (1.5)$$

we summarize in table I the critical behaviour and definitions of the critical indices. In sect. 2 we discuss the issue of triviality of the model. If it is indeed trivial (as all evidence points to) the critical exponents are those of mean field theory and there are non-leading logarithmic corrections. The exponents of these corrections are given in table I and depend on N of the group $O(N)$ [14, 83] ($N = 1$ for the one-component model).

The two definitions given for the renormalized charge agree in the continuum limit (sometimes one uses the continuum definition action with an extra factor 6: $\lambda_r = 3(m_r/\langle\varphi_r\rangle)^2$). Here Z denotes the field renormalization constant (and will be discussed in sect.3 in more detail) and not the partition function (sorry, but thats how it is). Only two of the critical exponents are independent (cf. e.g. [76]). The mean field values are for the scaling exponent of the correlation length $\nu = \frac{1}{2}$ and for the anomalous dimension $\eta = 0$. From the scaling relations we find $\alpha = 2 - d\nu = 0$, $\delta = \frac{d+2-\eta}{d-2+\eta} = 3$, $\gamma = \nu(2 - \eta) = 1$ and $\beta = \gamma/(\delta - 1) = \frac{1}{2}$.

1.3. Monte Carlo Methods

Quantization amounts to determination of expectation values

$$\langle A \rangle = \frac{1}{Z} \sum_{\Phi \in \Gamma} A(\Phi) \exp[S(\Phi)]. \quad (1.6)$$

TABLE I
Summary of the expected critical behaviour in the N -component model in terms of the reduced critical coupling $t \equiv (\kappa_c - \kappa)/\kappa_c$ and the external field j .

Order parameter		
$\langle \Phi \rangle$	$\sim t ^\beta \ln t ^{\frac{3}{N+8}}$	for $j = 0$
	$\sim j^{1/\delta} \ln j ^{\frac{1}{3}}$	for $t = 0$
Susceptibility		
$\chi = \langle \Phi(p=0)^2 \rangle_c = \frac{1}{ \Lambda } \sum_x \langle \Phi_0 \Phi_x \rangle_c$	$\sim t ^{-\gamma} \ln t ^{\frac{N+2}{N+8}}$	
Internal (link) energy		
$\langle E \rangle = \sum_{x,\mu} \langle \Phi_x \Phi_{x+\mu} \rangle$		
Specific heat		
$C_V = -\kappa^2 \frac{\partial \langle E \rangle}{\partial \kappa} = \frac{\kappa^2}{ \Lambda } (\langle E^2 \rangle - \langle E \rangle^2)$	$\sim t ^{-\alpha} \ln t ^{\frac{4-N}{N+8}}$	
Correlation length		
$\langle \Phi_0 \Phi_x \rangle_c \propto \exp(-m_r x)$	for $t \neq 0$	
	$\propto 1/ x ^{d-2+\eta}$	for $t = 0$
$m_r = 1/\xi$	$\sim t ^\nu \ln t ^{\frac{-N-2}{2N+16}}$	
Renormalized 4-pt coupling		
$\lambda_r = -\frac{\langle \Phi(p=0)^4 \rangle_c}{\langle \Phi(p=0)^2 \rangle_c^2}$		
or $= \frac{1}{2} (m_r / \langle \varphi_r \rangle)^2$	$\sim \ln t ^{-1}$	
where $\langle \varphi_r \rangle = \langle \varphi \rangle / \sqrt{Z}$		

In Monte Carlo integration one samples the field configurations with an equilibrium probability distribution $P(\Phi) \simeq \exp[S(\Phi)]$. This allows to determine expectation values according

$$\langle A \rangle = \lim_{T \rightarrow \infty} \frac{1}{T} \int_0^T d\tau A(\Phi(\tau)) = \lim_{N \rightarrow \infty} \frac{1}{N} \sum_{n=1}^N A(\Phi_n). \quad (1.7)$$

The stochastic variable is the field $\Phi(\tau)$ evolving with the stochastic (computer) time τ . It is determined from a homogeneous Markov process with transition probability T ,

$$P(\Phi_n = \varphi_n | \Phi_{n-1} = \varphi_{n-1}) = T_1(\varphi_n | \varphi_{n-1}) \quad (1.8)$$

i.e. T_k depends only on the numbers of time steps k but not on the history. If $T_k(\varphi'|\varphi) > 0$ for all pairs (φ', φ) and the process is aperiodic then it is ergodic. A Monte Carlo integration algorithm usually constructs such a Markov sequence of configurations, similar to a sequence of snap shot of some realistic ferromagnet. Thus the reason for calling the method a simulation. In realistic simulations ergodicity and the related problem of relaxation are important questions. In particular if there are topologically different sectors in configuration space some Monte Carlo updating algorithms may have problems connecting them.

If implemented correctly the Monte Carlo integration leads to correct results with a purely statistical error that decreases with the number of iterations like $1/\sqrt{N}$. The results are for finite size lattices, however. Control of both, the statistical error and the finite size effects, belongs to the central issues of this field.

One starts with an (arbitrary) configuration. The Markov sequence of configurations

$$\varphi_0 \rightarrow \varphi_1 \rightarrow \varphi_2 \rightarrow \dots \quad (1.9)$$

produces samples of the corresponding probability distributions, which, depending on certain sufficient conditions, approach the equilibrium distribution,

$$P^{(0)} \rightarrow P^{(1)} \rightarrow P^{(2)} \rightarrow \dots \rightarrow P \text{ (equilibrium distribution)}, \quad (1.10)$$

where $P^{(n)} = T^n P^{(0)}$. In a calculation one therefore starts to measure observables only after a sufficient number of “equilibrating” Monte Carlo steps. Subsequent updates then produce configurations according to the required distribution.

Meanwhile we have a collection of updating algorithms [145]. Some of them proceed by changing the configurations locally, i.e. just one variable at a time, others try to implement collective updates of nonlocal nature.

Local updating algorithms

- **Metropolis:** The simplest and oldest [107] algorithm; we discuss it below.
- **Heat bath:** Like an iterated Metropolis updating, optimizing the local acceptance rate.
- **Overrelaxation:** A sometimes very effective generalization of the heat bath algorithm.
- **Microcanonical:** Reformulates the updating in terms of a deterministic, discrete Hamiltonian evolution in a space with doubled number of variables: (Φ, Π) . A variant method introduces a microcanonical demon.
- **Hybrid Monte Carlo:** Combines a number of microcanonical updates (a “trajectory”) with a final Monte Carlo acceptance step.
- **Langevin:** Uses the stochastic differential equation for the construction of configurations; equivalence to the microcanonical and the hybrid method may be demonstrated (in certain limits).
- **Multicanonical:** Or multimagnetical or entropy sampling, samples an ensemble with modified energy density, particularly well suited for systems with degenerate ground states (like at 1st order phase transitions or in spin-glasses) [5, 6].

Non-local updating algorithms

- **Multigrid:** Employs scale changing transformations to identify possible collective updating modes, essentially a simultaneous updating on several length scales.
- **Cluster:** Identifies the system-specific dynamical nonlocal degrees of freedom; this method is very efficient for certain models and will be discussed below in more detail.

1.3.1. Metropolis Algorithm

Considering a stochastic process $X(\tau)$, detailed balance is a sufficient condition that the probability distribution approaches the equilibrium distribution $\exp[S(x)]$,

$$P_1(x|y)e^{S(y)} = P_1(y|x)e^{S(x)} \Rightarrow \lim_{\tau \rightarrow \infty} P(X(\tau) = x) \simeq e^{S(x)}. \quad (1.11)$$

Summation over x shows that the limiting distribution is an eigenvector of P_1 . The Metropolis algorithm [107], starting at some value x (i.e. some initial configuration), consists of the steps:

1. Choose some y according to some *a priori* transition probability $P_T(y|x)$.
2. Accept the new value y with the probability

$$P_A(y|x) = \min \left(1, \frac{P_T(x|y) \exp[S(y)]}{P_T(y|x) \exp[S(x)]} \right) \quad (1.12)$$

$$= \min(1, \exp[S(y) - S(x)]) \text{ for } P_T(x|y) = P_T(y|x). \quad (1.13)$$

It is straightforward to see, that the resulting $P_1 = P_T P_A$ fulfills detailed balance. In particular for symmetric P_T the information necessary to decide on acceptance or rejection comes only from the change of the action ΔS with regard to the change of the variable. If this change is local, i.e. just at some field variable Φ_x , the change of action may be determined from the field values in the local neighbourhood.

3. Repeat these steps from the begin.

One MC iteration is one sweep through the lattice, that is one attempt to update for each field variable on the lattice. Typical calculations perform $O(10^6)$ MC iterations for given lattice size and couplings constant values.

The exponential autocorrelation time controls the statistical dependence of subsequent configurations and may be defined

$$|P^{(n+1)} - P| \leq \exp(-1/\tau_{exp}) |P^{(n)} - P| \quad (1.14)$$

or from the autocorrelation of some observable A ,

$$\Gamma_A(n) = \langle A(\varphi_0)A(\varphi_n) \rangle - \langle A \rangle^2 \simeq \exp(-n/\tau_{exp,A}), \quad \tau_{exp,A} \equiv \sup_A \tau_{exp,A}, \quad (1.15)$$

or from the integrated autocorrelation time

$$\tau_{int,A} = \frac{1}{2} + \sum_{n>0} \frac{\Gamma_A(n)}{\Gamma_A(0)}. \quad (1.16)$$

The latter quantity controls directly the statistical error in estimates of $\langle A \rangle$; a run of n measurements contains only $n/2\tau_{int,A}$ effectively independent measurements. This relaxation behaviour affects particularly systems with large correlation lengths ξ (near critical points), since the autocorrelation length grows like

$$\tau_{exp} \simeq \min(L, \xi)^z, \quad \tau_{int,A} \simeq \min(L, \xi)^{z_A} \quad (1.17)$$

where z and z_A denote the dynamical critical exponents. They depend on the updating algorithm and have the value 2 for most local algorithms like the Metropolis algorithm (for overrelaxation algorithms this value may be smaller: ~ 1 [145]). The computational effort for the simulation of a system of linear extension L near a critical point², where $\xi \simeq L$, grows like L^{d+z_A} . This phenomenon is called *critical slowing down*. For more detailed discussions cf. [123, 124, 145].

In the MC simulation the statistical error of the measured quantities shrinks with the inverse square root of the number of statistically independent configurations. Improvement of the performance therefore can be achieved only by improving the updating algorithm by making them computationally simple (and quick), by reducing the autocorrelation time and by reducing the dynamical critical exponent z . This is the motivation for the introduction of multigrid- and cluster updating algorithms.

1.3.2. Cluster Algorithm

Fortuin and Kastelyn [81, 82] pointed out that the Ising model has an alternative formulation as a bond percolation model. This leads to clusters of connected bonds [23], which are the nonlocal dynamical objects of the Ising model.

Swendsen and Wang [131] suggested a very efficient updating algorithm based on alternating between the spin and the cluster representation. For a given spin configuration one first identifies Ising clusters built of neighboured sites with parallel spins. Some of the bonds are then deleted with probability $\exp(-2\kappa)$, the resulting bond clusters are the dynamical FK-CK-SW-Clusters [81, 23, 131]. With a probability 0.5 one now can flip simultaneously all spins in a cluster, repeating this for all clusters. This results in a new spin configuration and the updating step is completed (cf. fig. 2).

It turns out that this algorithm gives $z \simeq 0.3$ for the 2D and $z \simeq 1$ for the 4D Ising model. Wolff proposed a modification, where one randomly chooses a site and identifies the cluster connected to it like in the SW-algorithm; this cluster is then flipped unconditionally. This results in $z \simeq 0$ for the 4D system!

The cluster algorithm originally was designed for systems like the Ising or the Potts model, where the spin variables take values in a discrete group. Wolff [144] observed, that one may extend its scope of application to continuous groups, that have embedded Ising variables (the group manifold may be split into disjoint parts, cf. [124]), like e.g. the group $O(N)$. This allowed to utilize the updating method for N -component Φ^4 theories. The cluster method has provided a major breakthrough, the efficiency of the algorithm has brought forward results for scalar models with highest computational precision.

² For systems with several coexisting phases the autocorrelation length grows even exponentially with $\simeq \exp(cL^{d-1})$; multicanonical algorithms address this tunneling problem.

Fig. 2. The Swendsen-Wang cluster updating algorithm: $\{s\} \rightarrow \{b\} \rightarrow \{b'\} \rightarrow \{s'\}$.

The cluster representation allows the construction of observables with reduced variance, so-called *improved estimators* [127]. The propagator between spins at two sites, e.g., may be obtained by just counting how often both spins belong to the same cluster:

$$\langle \phi_x \phi_y \rangle = \left\langle \sum_{\text{all clusters } c} \chi_c(x) \chi_c(y) \right\rangle \quad \text{where} \quad \chi_c(x) = \begin{cases} 1 & \text{if } x \in c \\ 0 & \text{if } x \notin c \end{cases} . \quad (1.18)$$

For a given set of configurations this allows determination of the propagators for larger distances with much better statistical quality than achieved from the direct measurement.

The clusters are the dynamical objects of the critical system, a realization of Fisher's droplets. One therefore would expect relations between the geometrical properties and some critical indices. Due to scale invariance at a critical point clusters should look alike on different length scales. In quantum mechanics this is expressed by the fractal structure of the quantum paths, which are of Brownian nature. We might expect such a fractal structure also in the field configurations of quantum field theory (cf. fig. 3).

The relation between such a fractal structure and the odd critical index may be argued as follows [126]. Under a scale transformation we have scaling of the reduced critical temperature t (cf. table I) in the form

$$\xi \rightarrow b\xi, \quad t \rightarrow b^{-1/\nu} t \quad (1.19)$$

where ν denotes the scaling index of the correlation length. In a volume L^d the total magnetization scales according to table I

$$M(L) \propto L^d t^\beta \quad \rightarrow \quad (1.20)$$

$$M(bL) \propto (bL)^d b^{-\beta/\nu} t^\beta = b^{d-\beta/\nu} M(L) . \quad (1.21)$$

Fig. 3. A 3D cross section through a large cluster of a 4D Ising system near the critical point

We therefore expect finite size scaling of $M(L) \simeq L^{d-\beta/\nu}$, an anomalous dimension. This scaling behaviour should be followed by the clusters, as they are relevant for the critical behaviour. They should therefore exhibit a fractal dimension $d_f = d - \beta/\nu = d/(1 + 1/\delta)$. In 4D we expect mean field critical exponents $\delta = \frac{1}{3}$ and thus $d_f = 3$.

In a computer study on a finite lattice the clusters are of limited extension. Small clusters are essentially one-dimensional lattice animals, whereas large clusters will feel the boundaries and fill the space and then behave like d-dimensional objects. Scaling behaviour we can expect only at intermediate size clusters. However, the larger the lattice, the larger the domain of intermediate size. In a study of the 4D Φ^4 theory with $O(4)$ symmetry [80] the relation between mass s (number of sites belonging to the cluster) and size R (the square root of the mean square radius between points of the cluster) was studied.

In fig. 4 results of simulations for 4D lattices of various size demonstrate the existence of a scaling region. Its slope is the fractal exponent in the relation

$$s \propto R^{d_f} \tag{1.22}$$

with a value $d_f \approx 3.05$ indeed compatible with the expectations. An earlier study for the 3D Ising model [138] had produced a value $d_f = 2.51$ also compatible with the expected relation to the corresponding critical exponents in $d = 3$.

2. TRIVIALITY OF Φ^4

Fig. 4. In this log-log plot [80] of observed combinations (s, R) of clusters at the critical point the intermediate scaling region becomes obviously larger for larger lattices. Its slope defines the fractal dimension.

2.1. Rigorous Results

The claim “This theory is trivial” should be formulated more explicitly: Defining the continuum theory as the limit $a \rightarrow 0$ of the lattice theory, then all n -point functions may be expressed through products of 2-point functions (a theory of generalized free fields), which even may be those of a free particle (a theory of free fields).

Let me summarize here the main results. For more details one should refer to a review like [51, 20].

$D < 4$: The continuum limit defines an interacting field theory. The renormalized 4-point coupling λ_r is bounded ($0 \leq \lambda_r \leq \text{const}$) and perturbation theory applies (cf. [49, 50, 15] and further references in [20]).

$D > 4$: The continuum limit defines a trivial theory with mean field behaviour; all connected $2n$ -point functions (Wightman-distributions) vanish. Most likely this is a theory of free fields (cf. [1, 40, 16]).

$D = 4$: No rigorous proof of triviality exists, however there is a collection of results which leave little room for another result.

- Triviality has been conjectured by Wilson [141, 143] in the framework of perturbative renormalization group and, under this assumption, many scaling results have been derived (cf. [14]).
- The renormalized 4-point coupling λ_r is bounded ($0 \leq \lambda_r \leq \text{const}$); for the single component theory the critical exponents are bounded from below by gaussian (mean field) values [51].

- Considering the equivalence to random walks [132, 133] led to exact inequalities like $\lambda_r \leq 3p_{is}$ (where p_{is} denotes the intersection probability of 4D random walks) [1, 2, 3, 40, 28].
- Rigorous control of block spin transformations at the critical point (the massless theory) proves triviality for *small enough* λ_r [48]; close to the critical point there are logarithmic corrections [59, 60].

If the continuum limit is trivial and therefore defined by a fixed point of gaussian nature then its nature does not change in the complete $SU(2)$ gauge Higgs model [62] – although another additional FP at some different value cannot be excluded. *Assuming triviality* one can find regions, where the high temperature series (expansion in $1/\kappa$) still gives reliable results and the (renormalization group) scaling behaviour is already valid. This overlap allows to continue n -point functions from the symmetric (hot) phase through the phase transition [102]. Triviality implies a bound on the renormalized coupling and on the Higgs mass, even if the model is just an effective theory [19, 26]. We will discuss these issues below in more detail.

Fig. 5. Phase diagram of the 1- or (in parentheses) 4-component Φ^4 model

The phase diagram of the Φ^4 model in the (κ, λ) plane is sketched in fig.5. For the 1-component model one has a massive Higgs boson in both phases. At the phase transition the dimensionless mass vanishes due to $a \rightarrow 0$. The 4-component model has four degenerate massive bosons in the symmetric phase. In the broken phase one finds one massive boson and three massless Goldstone modes (although $a > 0$). The figure also gives regions of applicability of the standard perturbative and non-perturbative methods. Monte Carlo calculations cover the whole domain of interest

but they are limited to finite volume. On the other hand, the analytic methods are limited to certain domains and have to assume dominance of the gaussian fixed point (GFP). A thorough analytic understanding, however, helps to analyze the Monte Carlo results in a reliable way, as I try to demonstrate below.

Before we turn to Monte Carlo methods and results let us briefly review the results of renormalization group. Perturbation theory gives the β -function that describes the rescaling properties of the coupling with respect to a change of the scale μ . For the 1-component model the one-loop result is

$$\left(\frac{\partial\lambda}{\partial\ln\mu}\right) = \beta(\lambda) \equiv \frac{3}{16\pi^2}\lambda^2 + O(\lambda^3). \quad (2.1)$$

Solution of the differential equation gives

$$\lambda(\mu) = \frac{\lambda(\Lambda)}{1 - \lambda(\Lambda)\frac{3}{16\pi^2}\ln(\mu/\Lambda)} \quad \text{or} \quad \lambda(\Lambda) = \frac{\lambda(\mu)}{1 + \lambda(\mu)\frac{3}{16\pi^2}\ln(\mu/\Lambda)}. \quad (2.2)$$

The cutoff Λ corresponds to the inverse lattice spacing $1/a$, thus $\lambda(\Lambda) = \lambda_{bare}$. For the physical scale μ one could choose some low-energy mass (like the Higgs mass), thus $\lambda(\mu) = \lambda_r$. Taking these results at face value, for fixed $\lambda(\mu)$ the cutoff Λ cannot be pushed to arbitrary high values due to a zero in the denominator (Landau pole). Or, to rephrase this problem as a question: How large do we have to make the microscopical coupling λ_{bare} in order to have a non-zero macroscopical coupling λ_r ?

Fig. 6. The renormalization of the quartic coupling as expected from renormalization group arguments.

In fig.6 this situation is summarized. Trajectories of fixed bare coupling are bounded from above by the $\lambda_{bare} = \infty$ values of λ_r . Holding λ_r fixed but attempting to raise the cutoff (approach the critical point, i.e. the continuum limit) is not possible - one gets stuck at the upper bound at some value of Λ (or, equivalently, at some non-zero value of $a(\kappa) > 0$). The bound forces the renormalized coupling to approach zero in the continuum limit. Only at finite cutoff non-vanishing values of λ_r are permitted. Thus even a trivial theory may have an effective interaction below the cutoff.

This discussion is based on the one-loop perturbative result and the renormalization group equations. It was one of the challenges of the Monte Carlo approach to confirm (or not confirm) this scenario. Although the asymptotic shape of the upper bound is given, the multiplicative factor is of non-perturbative nature. Also, the shape at small values of Λ is regularization dependent. The corresponding amplitudes are universal up to regularization dependent corrections $O(\mu^2/\Lambda^2)$.

In a sensible regularization the cutoff should be larger than the masses of the physical states, thus $\Lambda/\mu > 1$. If the situation is like discussed above, this provides an upper bound on λ_r . Perturbation theory in the electro-weak gauge coupling g relates the renormalized coupling with the ratio between the Higgs mass m_H and the mass of the heavy vector boson W ,

$$\lambda_r = \frac{1}{2}R^2, \quad R = \frac{m_H}{F} = \frac{g}{2} \frac{m_H}{m_W}, \quad F \equiv \langle \varphi \rangle / \sqrt{Z}. \quad (2.3)$$

(As mentioned, sometimes the continuum notation with an extra factor 6 is used: $\lambda_r = 3R^2$, cf. table I.) Given the experimental values ($F \simeq 246$ GeV, or $m_W = 80.6(4)$ GeV, $g^2 \simeq 0.4$) the non-perturbative upper bound on the renormalized 4-point coupling provides an upper bound on the Higgs mass [19, 26], unrelated to the usual unitarity-bound.

What evidence can we expect from Monte Carlo simulations? There are three groups of results

- (a) Phase structure and critical exponents, derived from bulk quantities like the internal energy, susceptibility or specific heat; detailed investigation of the finite size properties of the partition function allows quantitative statements on finite size scaling, the thermodynamic limit and logarithmic corrections.
- (b) Monte Carlo renormalization group (MCRG) methods allow to determine the flow of coupling and the fixed point structure, including the critical exponents.
- (c) Propagator measurements lead to the mass spectrum and values of the renormalized couplings. These results are of particular interest concerning the triviality bound on the Higgs mass and its regularization dependence. The energy spectrum also allows the determination of phase shifts.

In the subsequent discussion of this section I first present more qualitative results from real space renormalization group, then a high precision determination of the partition function and the logarithmic corrections. In sect. 3 the non-perturbative results on the bound are discussed.

2.2. Real Space Renormalization Group

In perturbative renormalization group the number of couplings considered is very small, although the number of couplings generated in the transformation may be infinite. The Monte Carlo renormalization group method, also called real space renormalization group (RSRG) method since it works in position space, allows to deal with a larger coupling space, although one has to truncate as well.

The *Scaling Hypothesis* suggests, that the singularities of the thermodynamic quantities are due to the divergence of the correlation length [37, 4, 22]. At the critical point the system should be scale invariant and under scale changing trans-

formations

$$Z(\Lambda) \xrightarrow{T(\Lambda, \Lambda')} Z'(\Lambda') \quad (2.4)$$

the physical properties (i.e. the properties at long distance in terms of lattice spacing) and thus the partition function should be invariant. Here the transformation T is element of a semigroup. On a lattice it is realized by the Wilson-Kadanoff *block-spin transformation* [143], where the local degrees of freedom are “integrated out”. We have

scale transformation	Λ	\rightarrow	Λ'
linear factor b	$ \Lambda / \Lambda' $	$=$	b^D
invariance	$Z(\Lambda)$	$=$	$Z'(\Lambda')$
field variables	$\Phi \in \Gamma$	\rightarrow	$\Phi' \in \Gamma'$
correlation length	$n_\xi a$	\rightarrow	$n'_\xi a' = (n_\xi/b)ba$

For lattice systems T transforms an ensemble of configurations on Λ into an ensemble of configurations on Λ' . The correlation length changes by the scale factor b .

Given that the original ensemble was distributed according to a Gibbs measure for an action $S(\kappa, \Phi)$ let us for the moment assume that the blocked ensemble also follows such a measure, but for a different action $S(\kappa', \Phi')$ (cf. the discussion further down). Let us formulate the BST (block spin transformation) $\Phi \rightarrow \Phi'$ by introducing a normalized transformation probability P with the properties

- (a) normalization: $\int d\mu_{\Lambda'}(\Phi') P(\Phi', \Phi) = 1$
- (b) positivity: $P(\Phi', \Phi) \geq 0$; with (a) this implies that for all Φ there is a Φ' such that $P(\Phi', \Phi) \neq 0$, i.e. there is a non-vanishing probability of mapping into each sector of Γ' .
- (c) symmetry: all symmetries of the action S should be respected.

We then may describe the transformation by

$$\begin{aligned} Z(\Lambda) &= \int d\mu_\Lambda(\Phi) \exp[S(\kappa, \Phi)] = \int d\mu_\Lambda(\Phi) d\mu_{\Lambda'}(\Phi') P(\Phi', \Phi) \exp[S(\kappa, \Phi)] \\ &\equiv \int d\mu_{\Lambda'}(\Phi') \exp[S(\kappa', \Phi')] = Z'(\Lambda') \end{aligned} \quad (2.5)$$

with

$$\exp[S(\kappa', \Phi')] = \int d\mu_\Lambda(\Phi) P(\Phi', \Phi) \exp[S(\kappa, \Phi)]. \quad (2.6)$$

The BST is largely arbitrary [17] and may be chosen optimal from the point of view of simulational simplicity. One has considered both, deterministic and probabilistic forms,

$$\begin{aligned} P(\Phi', \Phi) &= \prod_{x'} \delta(\Phi'_{x'}, f_{x'}(\Phi)) && \text{(deterministic),} \\ &= \prod_{x'} \exp(\Phi'_{x'} \sum_\alpha \rho_\alpha f_{x'}^\alpha(\Phi)) && \text{(probabilistic).} \end{aligned} \quad (2.7)$$

A deterministic transformation with a linear relation between the spins and the blockspins makes the new spin at x' an average over the old spins within some block

$B_{x'}$,

$$f_{x'}(\Phi) \propto \sum_{x \in B_{x'}} \Phi_x, \quad (2.8)$$

whereas a nonlinear form could be chosen to keep certain expectation values (in the example below: $\langle \Phi^2 \rangle$) fixed during the transformation,

$$f_{x'}(\Phi) = \text{sign} \left[\sum_{x \in B_{x'}} \Phi_x \right] \frac{1}{16} \sum_{x \in B_{x'}} \Phi_x^2. \quad (2.9)$$

For Ising spin systems this choice gives the majority rule. Probabilistic transformations have adjustable parameters ρ_α that may be used to optimize certain features.

Under repeated transformations the (dimensionless) correlation length shrinks and the equivalent action changes.

$$n_\xi \rightarrow n'_\xi \rightarrow n''_\xi \rightarrow \dots \quad n_\xi^* = \begin{cases} 0 & \text{trivial FP} \\ \infty & \text{critical FP} \end{cases}, \quad (2.10)$$

$$\kappa \rightarrow \kappa' \rightarrow \kappa'' \rightarrow \dots \quad \kappa^* \quad (\text{fixed point}). \quad (2.11)$$

The couplings renormalize according

$$\kappa' = \kappa'(\kappa) \quad (2.12)$$

which serves as the definition of the BST in action space, and, assuming simple FP (fixed point) properties, $\kappa^* = \kappa'(\kappa^*)$. If we start at a critical point, the correlation length is infinite all the way: One stays on the critical hypersurface. If the correlation length was finite it will approach zero in the iteration of the BST, corresponding to the approach to a trivial (hot or cold) FP.

At the FP we may linearize (2.12) to obtain

$$\kappa'_\alpha(\kappa) = \kappa_\alpha^* + T_{\alpha\beta}^*(\kappa - \kappa^*)_\beta + o(\|\kappa - \kappa^*\|) \quad \text{with} \quad T_{\alpha\beta} = \left(\frac{\partial \kappa'_\alpha}{\partial \kappa_\beta} \right)_{\kappa^*} \quad (2.13)$$

or, for the n-th step

$$T_{\alpha\beta}^{(n+1,n)} = \frac{\partial \kappa_\alpha^{(n+1)}}{\partial \kappa_\beta^{(n)}} \rightarrow T_{\alpha\beta}^*. \quad (2.14)$$

The eigenvalues $\{\lambda\}$ of the FP values of the linearized BST decide on the number of relevant ($\lambda > 1$), marginal ($\lambda = 1$), or irrelevant ($\lambda < 1$) operators (couplings) at the critical FP. (There may also be redundant operators. They occur e.g. if the set of couplings is overcomplete [109, 58]). Fig. 7 shows an example for the RG flow. Starting at the FP with a small perturbation, the flow will lead away into the direction of relevant operators. This defines the renormalized trajectory, along which there are no contributions of irrelevant operators, i.e. no corrections to scaling.

Usually almost all couplings (corresponding operators in the action) are irrelevant. The attraction domain of a FP is high-dimensional and only a few (two or three) coupling are relevant. This behaviour is the reason for universality classes: The same critical surface is domain of attraction for many different initial actions.

Fig. 7. Schematic display of the renormalization flow in coupling space; starting from the vertical axis at $\kappa_2 = 0$

Although the position of the critical points may be different, the critical behaviour is not, as it is always given by the properties of T^* .

The linearized BST T^* factorizes into even and odd subspaces, depending on the symmetry properties of the corresponding terms in the action under reflection $\Phi \leftrightarrow -\Phi$. The relevant eigenvalues are related to the corresponding critical exponent. This may be seen from the scaling behaviour of e.g. the correlation length. Assuming that its critical behaviour is given by some critical index ν we find

$$\begin{aligned} \xi(\kappa) &= b\xi'(\kappa'(\kappa)) \rightarrow \\ (\kappa - \kappa^*)^{-\nu} &= b(\kappa'(\kappa) - \kappa^*)^{-\nu} = b\lambda^{-\nu}(\kappa - \kappa^*)^{-\nu} \end{aligned} \quad (2.15)$$

which is consistent only for

$$\nu = \frac{\ln b}{\ln \lambda}. \quad (2.16)$$

If there are marginal eigenvalues there is a line of FPs in the critical surface.

The position of the FP on the critical surface may depend on details of the BST [130]. In particular it may be moved into directions of redundant operators [38]. In practice the amount of redundancy is often not clear. Improvement may be desirable for both, the FP action (cf. [58]) and the renormalized trajectory [130, 47, 92]. Recent attempts to optimize the BST such that the FP action becomes particularly simple and as local as possible seem to be promising for asymptotically free theories [69].

Before I continue, let me mention possible difficulties and caveats.

- The transformation may introduce spurious singularities as discussed by Griffiths and Pearce [56, 57].
- Some BSTs at first order transitions may produce non-Gibbsian measures ([136, 137], cf. however [106]).
- The FP may describe a nonlocal action (no exponential damping of nonlocal terms) or it may be at infinity in the parameter space of the action.
- Depending on the lattice geometry and dimensions only a limited range of blocking factors is available.

- Like in perturbative renormalization group the number of couplings generated in the transformation may be infinite. In practical calculations one therefore has to rely on truncations.

For the following discussion we write the action as a sum of operators,

$$S = \sum_{\alpha} \kappa_{\alpha} S_{\alpha} . \quad (2.17)$$

Expectation values and correlators are related to derivatives of the free energy

$$\frac{\partial F}{\partial \kappa_{\alpha}} = \langle S_{\alpha} \rangle , \quad \frac{\partial^2 F}{\partial \kappa_{\alpha} \partial \kappa_{\beta}} = \frac{\partial \langle S_{\alpha} \rangle}{\partial \kappa_{\beta}} = \langle S_{\alpha} S_{\beta} \rangle - \langle S_{\alpha} \rangle \langle S_{\beta} \rangle . \quad (2.18)$$

BSTs provide different possibilities to obtain information on the critical properties.

Critical exponents: The cross-correlations between observables measured on the original and the blocked configurations allow to get estimators for the truncated T -matrix [105, 128].

$$\frac{\partial \langle S_{\alpha}^{(n+1)} \rangle}{\partial \kappa_{\beta}^{(n)}} = \sum_{\gamma} \frac{\partial \langle S_{\alpha}^{(n+1)} \rangle}{\partial \kappa_{\gamma}^{(n+1)}} \frac{\partial \kappa_{\gamma}^{(n+1)}}{\partial \kappa_{\beta}^{(n)}} = \sum_{\gamma} \frac{\partial \langle S_{\alpha}^{(n+1)} \rangle}{\partial \kappa_{\gamma}^{(n+1)}} T_{\gamma\beta}^{(n+1,n)} , \quad (2.19)$$

$$\frac{\partial \langle S_{\alpha}^{(n)} \rangle}{\partial \kappa_{\beta}^{(m)}} = \langle S_{\alpha}^{(n)} S_{\beta}^{(m)} \rangle - \langle S_{\alpha}^{(n)} \rangle \langle S_{\beta}^{(m)} \rangle . \quad (2.20)$$

Here T is obtained from (2.19) by inversion. Due to the truncation there will be inherent errors (see however [121]). This approach has been very successful for 2D and 3D spin models where it has provided the maybe best estimates of critical exponents [18].

Flow in the space of observables: Repeated BST leads one to the renormalized trajectory. Matching of observables allows to relate couplings of different simulations.

Flow in the space of couplings: This would allow to identify FPs and universality class in a very intuitive and direct way.

Unlike in perturbation theory, in non-perturbative RSRG calculations it is no straightforward task to measure renormalized couplings. It is simple to construct the blocked configurations (in position space), but one has no direct means to know about the corresponding action. There is the problem to learn the values of (many, in the thermodynamic case infinitely many) couplings of the blocked action, which is not known directly. A possibility is by operator matching: Matching the observables determined by Monte Carlo simulations on lattices of the size of the blocked lattice [122, 75, 63, 12]. However, for this one has to combine statistically independently determined expectation values which needs high statistics. Another, very efficient method has been suggested by Swendsen [129] and amounts to determine conditional expectation values in the background of given configurations.

MCRG calculation for the one component Φ^4 model have been performed on lattices up to size 16^4 and the results were compatible with the expected scenario: one relevant even and one relevant odd direction in operator space. The result for the even critical exponent was good ($\nu = 0.53(4)$ from e.g. [11, 90], or from [21]) but the statistical accuracy not sufficient to identify the expected next-to-leading marginal eigenvalue. No convincing signal for logarithmic corrections could be determined in those calculations.

However, from the flow structure of the renormalized couplings one could try to find out, whether different values of the bare quartic coupling are in one universality class. This was done in [90] in a space 24 different couplings corresponding to 6 quadratic (local and distance 1, 2, 3, and 4 spin-spin products) and 18 quartic (local and neighbouring 2-, 3- and 4-spin products) operators. The simulation was done on a 16^4 lattice with most of the initial couplings set to zero. Only the nearest-neighbour coupling κ and the bare 4-point coupling λ were non-zero. For given fixed values of λ (0.2, 0.4 and 2) the model was simulated for the critical value of κ and BSTs were performed down to lattices of size 8^4 and 4^4 . The renormalized couplings in the 24D space were determined with Swendsen's method [129].

Fig. 8. Flow structure in coupling space; starting on the critical surface in the (κ_1, κ_2) plane (corresponding to the bare quartic coupling and n.n. coupling) the RG flow moves towards a common FP, independent of the bare quartic coupling: it is irrelevant.

The observed flow may be summarized as in fig. 8. From different starting values of the bare quartic coupling on the critical surface the flow is towards a common FP. In the study different BSTs were considered. As the FP position may depend on the particular BST one could expect different flow structure, which indeed was observed [21, 89, 90]. The deterministic nonlinear type of BST discussed above produced a flow towards the FP characteristic for the Ising system. The overall result demonstrated, that the bare quartic coupling is not relevant for the FP and thus for the continuum theory – in agreement with the notion of triviality.

2.2.1. Critical Indices from Bulk Quantities

Bulk quantities like the internal energy per link $\langle E \rangle$ or the magnetization $\langle \Phi \rangle$ are the most direct way to the determination of scaling behaviour. However, they are

affected by finite size effects and therefore the critical exponents may be masked behind the smooth crossover between the phases typical for finite systems. Finite size scaling [10, 4] relates finite size properties with the critical exponents in the thermodynamic limit. However, usually one needs very precise determination of the quantities involved. The histogram method, an old idea [30] reshaped into the multi-histogram approach by Ferrenberg and Swendsen [31, 32, 33], allows to combine measurements at different couplings in an efficient way.

We rewrite the partition function in terms of the density of states (for simplicity we assume that the set of energy values is discrete, otherwise we have to rely on some binning of the allowed range).

$$\begin{aligned} Z(\kappa) &= \int d\mu_\Lambda(\Phi) \exp[\kappa S(\Phi)] = \int d\mu_\Lambda(\Phi) \sum_E \delta(S - E) \exp[\kappa S(\Phi)] \\ &= \sum_E \rho(E) \exp(\kappa E) = \sum_E p(E|\kappa) . \end{aligned} \quad (2.21)$$

The probability for a configuration having the total action E for coupling κ is $p(E|\kappa)$ and is estimated by the corresponding histogram values $h(\kappa, E)$ obtained in the Monte Carlo simulation of the system. Simulations at different values of the coupling provide different estimators for the spectral density $\rho(E)$:

$$\begin{aligned} \kappa_0 &\rightarrow \rho_0(E) = h(\kappa_0, E) \exp(-\kappa_0 E) , \\ \kappa_1 &\rightarrow \rho_1(E) = h(\kappa_1, E) \exp(-\kappa_1 E) , \quad \text{etc.} \end{aligned} \quad (2.22)$$

However, the statistical accuracy for these different estimators will be best for those values of E close to the corresponding expectation value (i.e. near the peak of the corresponding histogram). A suitable combination of histograms [31, 32, 33], however, gives a reliable estimator over a broader range of energies (and therefore couplings). From this estimator for the spectral density one may construct energy histograms at arbitrary values of the coupling, as in fig. 9.

This technique may be generalized to other observables and terms in the action. Taking into account energy and magnetization we have the partition function

$$Z(\kappa, h) = \sum_{E, M} \rho(E, M) \exp(\kappa E + hM) \quad (2.23)$$

allowing the precise determination of expectation values of arbitrary functions of E and M ,

$$\langle f(E, M) \rangle = \frac{1}{Z} \sum_{E, M} \rho(E, M) f(E, M) \exp(\kappa E + hM) . \quad (2.24)$$

An example is the specific heat C_V ; in fig. 10 both, the values determined at specific couplings and the continuous curve from the multi-histogram analysis is shown. Each curve contains all the information of the corresponding individual couplings (for that lattice size).

The representation (2.23) also allows for analytic continuation to complex values of κ and h since only the exponential has to be continued. One therefore can determine the zeroes of Z in the complex κ and h planes. In the actual calculation

Fig. 9. The logarithm of the probability distribution (histogram) as reconstructed from the multihistogram: $\ln[\rho(E)e^{\kappa_0 E}]$ vs. E , for $\kappa_0 = 0.15055$ and lattice size 16^4 .

Fig. 10. The specific heat C_V for the one-component Φ^4 model determined for lattice sizes 8^4 , 12^4 , 16^4 , 20^4 , and 24^4 (from [84]).

this can be done reliably only close to the values of the couplings, where the original histograms have been determined, otherwise the statistical errors of the estimated spectral density blow up and lead to large uncertainties. Experience shows, that extrapolation is feasible in an elliptical domain with the real positions of measurements between the foci of the principal axis.

The study of zeroes of the partition function has been started by Lee and Yang [146, 147]; zeroes in the complex external field h are called Lee-Yang zeroes. They have to lie at purely imaginary values of h (on the unit circle in the fugacity $z = e^{-2h}$ plane) [146, 147]. Zeroes in the even coupling (the temperature) have been studied

in particular by Fisher [36] and are thus usually called Fisher zeroes. On a finite lattice the partition function is a finite-degree polynomial in $e^{-4\kappa}$ and z .

Fig. 11. **Left:** Finite size scaling behaviour of the imaginary part of the closest Fisher-zero κ_1 for lattice size $L = 8, 12, 16, 20$ and 24 at $h = 0$. (a) The leading exponent is related to the slope of the straight line and a fit gives $-2.088(6)$ slightly differing from the mean field expectation $-1/\nu = -2$. This difference is due to the presence of logarithmic corrections as demonstrated in (b) where the leading behaviour has been cancelled by considering $L^2 \text{Im}\kappa_1$. **Right:** Finite size scaling behaviour of the imaginary part of the closest Lee-Yang-zero h_1 for lattice size $L = 8, 12, 16, 20$ and 24 and $\kappa = 0.149703$. (a) The leading exponent is related to the slope of the straight line and a fit gives $-3.083(4)$ slightly differing from the mean field expectation $-1/\delta = -3$. This difference is due to the presence of logarithmic corrections as demonstrated in (b) where the leading behaviour has been cancelled by considering $L^3 \text{Im}h_1$ (figures from [86]).

Expressing, e.g. Z through a product of zeroes we find, that the specific heat – the second derivative of its logarithm – is peaked for those real values of κ that are closest to a nearby complex zero:

$$Z \propto \prod_i (\kappa - \kappa_i) \quad \rightarrow \quad C_V(\kappa) \propto \sum_i \frac{1}{(\kappa - \kappa_i)^2} . \quad (2.25)$$

In the thermodynamic limit the zeroes accumulate and pinch the real κ -axis (and, for critical coupling, the real point $h = 0$): They build the critical singularity. The Λ -dependence of the positions of the zeroes closest to the real coupling axis can be related to the thermodynamic critical exponents (finite size scaling) and the logarithmic corrections.

Assuming that the gaussian FP controls the leading critical behaviour, perturbative renormalization group methods may be applied to predict the critical properties [14] and the finite size scaling behaviour of the partition function zeroes [13]. For the one-component Φ^4 model this was done recently [84, 86, 85] (for the $O(N)$ model cf. [83]) with the following results for the Fisher zeroes (using the reduced coupling t) and the Lee-Yang zeroes:

$$|t_j| \sim L^{-2}(\ln L)^{-\frac{1}{6}}, \quad (2.26)$$

$$|h_j| \sim L^{-3}(\ln L)^{-\frac{1}{4}}. \quad (2.27)$$

Here the leading exponents are the negative inverse of the mean field values for ν and δ , the multiplicative logarithmic corrections depend on the number of components of Φ and have other values for the N -component model. This result also gives the finite size scaling behaviour for the peak values of the specific heat and the susceptibility

$$c_L(t=h=0) \sim (\ln L)^{\frac{1}{3}}, \quad (2.28)$$

$$\chi_L(t=h=0) \sim L^2(\ln L)^{\frac{1}{2}}. \quad (2.29)$$

In a high statistics simulation the multi-histogram techniques were used to study bulk quantities of the Φ^4 model and the positions of the closest partition function zeroes [84, 86, 85]. The numerical result together with the Ferrenberg-Swendsen technique allowed sufficient precision to identify both, the leading critical exponent and the form of the logarithmic correction. The results for the Lee-Yang and for the Fisher-zeroes (cf. fig. 11) confirmed the expectation. The leading even and odd exponents agree with the mean field result. The logarithmic corrections are in good agreement with the expressions (2.26) and (2.27) derived on ground of perturbative renormalization group.

3. CONSEQUENCES OF TRIVIALITY

Let us now concentrate on results derivable under the impact of triviality like the bound on the renormalized coupling and the Higgs mass. We therefore discuss in this section in particular the $O(4)$ model because of its close relationship to the unified theory of electro-weak interaction. The notation refers to the lattice action (1.3) given above.

3.1. Results from Non-Monte Carlo Techniques

Using a local potential approximation and Wilson recursion relation technique for renormalization group calculations Hasenfratz and Nager [68] obtained analytic and non-perturbative results on the bound for the one-component model. The effect of the inherent approximations is hard to judge in that approach. A real breakthrough, however, were the results of Lüscher and Weisz [100, 101, 102] and for this reason I want to briefly summarize them.

The authors study the $N(\geq 1)$ -component model on a hypercubic lattice. Starting from the symmetric phase they proceed as follows (cf. fig. 5):

Symmetric phase: The high temperature (small κ) expansion for the renormalized mass m_r , coupling λ_r and the critical value κ_c is determined up to $O(\kappa^{14})$. The

values seem to be reliable up to relatively small values of $m_r \simeq 0.5$, already within the scaling region.

Scaling (critical) region: Here one uses the results of perturbation theory in the renormalized quantities: m_r and $\lambda_r(\kappa, \lambda)$ for fixed bare λ , using 3-loop β -functions. One has to assume that the gaussian FP defines the universality class. The a priori unknown integration constants like C_1 in

$$\kappa < \kappa_c : am_r(\lambda) = C_1(\lambda)(\beta_1 \lambda_r)^{-\beta_2/\beta_1^2} \exp\left(-\frac{1}{\beta_1 \lambda_r}\right) \{1 + O(\lambda_r)\} \quad (3.1)$$

contain the non-perturbative information and are taken from the κ -expansion values in the overlap region. Corrections to scaling are $O(a^2(\ln a)^c)$. The scaling form is used to continued through the phase transition to the phase with broken symmetry in a region $m_r \leq 0.5$.

Broken symmetry phase: The Integration constants below and above the critical point are related through the massless theory at the critical point,

$$\kappa > \kappa_c : C_1'(\lambda) = e^{\frac{1}{\beta_1}} C_1(\lambda) . \quad (3.2)$$

They are renormalization prescription dependent.

Fig. 12. Quantitative plot of renormalization group trajectories for the $O(4)$ model (from [102]). The abscissa variable $\bar{\lambda}$ corresponds to values of the bare coupling $0 \leq \lambda \leq \infty$. The range of κ -values roughly covers the scaling region $|m_r| \leq 0.5$. The curves correspond to constant renormalized 4-point coupling – they approach the critical line, but they never touch it: In the continuum limit one is forced to vanishing values of λ_r .

This program exploits standard analytic techniques in a very efficient way and worked nicely [100, 101, 102]. In fig. 12 trajectories of constant renormalized 4-point coupling are shown: They never cross the critical line, therefore only a non-interacting continuum limit is feasible.

We summarize the restrictions or assumptions for this approach:

- the κ -series is truncated;
- triviality (gaussian FP) is assumed;
- validity of perturbation theory in the renormalized couplings (renormalization group at the 3-loop level) is assumed.

Direct Monte Carlo simulations can check these assumptions and confirm the validity of the approximations. They also can determine further results concerning, for instance, the regularization dependence. A consistent picture gives weight to both, the analytical and the numerical approach.

3.2. Monte Carlo Simulations

First results go back to 1984 [140, 135] but stayed widely unnoticed. Only with the very high statistics studies of various groups [65, 108, 87, 88, 7, 74] since 1987 the results became convincing enough. These studies worked with lattice sizes up to 16^4 . Most results have been obtained in the broken phase, both for $j = 0$ and $j > 0$. Typically several 100.000 sweeps and measurements per point have been performed, using first the Metropolis, later the cluster algorithm. In summary thousands of hours supercomputer CPU-time (like e.g. Cray-YMP or equivalent) have been spent for these analyses. Some studies were concerned with the one-component model but, again, most concentrated on the $O(4)$ model.

For the determination of the renormalized coupling in the phase of broken symmetry we need (cf. (2.3) and table I)

- The vacuum expectation value $\Sigma = \langle \varphi \rangle$; the complication is, that for $j = 0$ in finite volumes there is no spontaneous symmetry breaking and one has to consider suitable definitions.
- The field renormalization constant Z or, equivalently, the *pion decay constant* $F \equiv \Sigma/\sqrt{Z}$. This may be determined e.g. from the propagators of the massless Goldstone modes.
- The renormalized mass m_r of the massive (Higgs) mode, determined from the measured Higgs propagator.

In addition to these quantities necessary for the derivation of λ_r we may also want to identify clear signals for the existence of Goldstone modes, like e.g. propagators at $j = 0$ and $j > 0$, just to be sure that the symmetry breaking mechanism is the conjectured one.

The problem to define, what one means by spontaneous symmetry on finite lattices, turned out to be hard in practice. A straightforward definition originally employed was

$$\Sigma = \langle |\overline{\varphi}^\alpha| \rangle \quad \text{where} \quad \overline{\varphi}^\alpha = \frac{1}{|\Lambda|} \sum_x \varphi_x^\alpha, \quad (3.3)$$

and m_r , F and Z were determined from the propagators of the field components parallel and perpendicular to the value $\overline{\varphi}^\alpha$ of the corresponding configuration, which meandered around in the $O(N - 1)$ subspace. That seemed to work nicely. In fig. 13 we show results for the Higgs mass determined that way on lattices of various size. Further results showed that the field renormalization constant stays close to the value 0.97 from the PT up to $m_r \approx 1$.

Fig. 13. The dimensionless renormalized Higgs mass $a(\kappa)m_r$, determined on lattices of various size and extrapolated to infinite lattice size (from [113]).

A better understanding of the infinite volume limit of the *ad hoc* ansatz (3.3) was important to achieve systematically improved quality of the results for Σ . Now, for $j \neq 0$ the symmetry is broken explicitly, all quantities are well defined and can be measured without reference to spontaneous symmetry breaking. For small values of the external field the would-be Goldstone states are still very light and therefore they feel the finiteness of the volume best. We have a situation of two different kinds of long correlation lengths (fig. 14). At the 2nd order PT $a(\kappa)m_r \rightarrow 0$, because $a(\kappa) \rightarrow 0$ for $\kappa \rightarrow \kappa_c$, since the theory is critical. Along the 1st order PT $a(\kappa)m_G(j) \rightarrow 0$ because the Goldstone boson mass $m_G(j) \rightarrow 0$ for $j \rightarrow 0$. In the discussion below we will denote masses of the massive mode m_σ and of the Goldstone mode m_π in analogy to the nonlinear σ -model.

Fig. 14. Phase structure in the (κ, j) -plane.

Let us recall again the important parameters of the model. The field Φ^α has four real components. In the symmetric (high temperature) phase the particle spectrum has 4 degenerate states. In the low temperature phase $\kappa > \kappa_c$, at infinite volume $O(4)$ symmetry is spontaneously broken. In this phase

$$\langle \varphi_x^0 \rangle = \Sigma, \quad \langle \varphi_x^i \rangle = 0 \quad (i = 1, 2, 3). \quad (3.4)$$

Here the spectrum of the theory contains three massless Goldstone bosons corresponding to the excitations in the $O(4)$ directions $\alpha = i = 1, 2, 3$. Therefore, the correlation functions do not fall off exponentially at large distances, but with an inverse power of the distance. Specifically, the Goldstone boson two-point function satisfies

$$\lim_{|x-y| \rightarrow \infty} 4\pi^2 |x-y|^2 \langle \varphi_x^i \varphi_y^j \rangle = Z \delta^{ij}. \quad (3.5)$$

For $O(4)$ symmetry the model contains six currents, all conserved at $j = 0$, whose charges generate the group. The corresponding Ward identities strongly constrain the behaviour of the correlation functions at large distances. In fact, the asymptotic behaviour of all the Green functions associated with the currents and with the fields φ_x^α is determined by the two low energy constants Σ and F [41]. In analogy with QCD, F is often referred to as the pion decay constant. It specifies the matrix elements of the axial currents $A_\mu^j(x)$ (in Minkowski space) between the ground state and single Goldstone boson states,

$$\langle 0 | A_\mu^j(0) | \pi^k(p) \rangle = i \delta^{jk} p_\mu F. \quad (3.6)$$

The low energy constants Z , Σ and F are related through

$$F = \Sigma / \sqrt{Z}. \quad (3.7)$$

For $j > 0$ the Goldstone boson mass m_π has a non-vanishing value which in the lowest order of chiral perturbation theory is

$$m_\pi^2 = j \frac{\Sigma}{F^2}. \quad (3.8)$$

Whenever (almost) massless states dominate the system the low energy (long distance) structure is of a universal character determined by the symmetries of the dynamics in terms of a few low energy constants and by the geometry of the finite system. One therefore may study an effective field theory with only Goldstone modes and the symmetry structure of the underlying model $O(N) \rightarrow O(N-1)$ [95, 43, 67, 111]. The effective Lagrangian has the same symmetry as the original system but is simple enough to permit a *systematic* perturbative expansion. It has the form

$$L_{\text{eff}} = \frac{1}{2} F^2 (\partial_\mu \vec{S} \partial_\mu \vec{S}) - \Sigma \vec{H} \vec{S} \\ + \text{further terms of higher order in } \vec{H} \text{ and } \vec{S}, \quad (3.9)$$

$$Z(\vec{H}) = \int d\mu(\vec{S}) \exp\left(\int dx L_{\text{eff}}\right). \quad (3.10)$$

In higher orders of this perturbative Lagrangian some further low energy constants Λ_Σ , Λ_F and Λ_M are required [67]. They are the scale parameters determining the logarithmic dependence of Σ , F and m_π on j . In systems of finite size L this expansion amounts to an expansion in powers of L^{-2} . It is reliable because the interaction between the Goldstone modes is weak at low momenta.

The first application of this idea [42, 95] has been made in the context of the study of finite size effects in QCD with light quarks, whose low energy properties are determined by the chiral $SU(2) \otimes SU(2) \simeq O(4)$ symmetry [41]. Therefore one refers to this approach as "chiral perturbation theory". A comprehensive description can be found in [43, 94, 67].

The effective theory and its expansion relates values of quantities determined at finite volumes and $j > 0$ with those at $j = 0$ at infinite volume,

$$\Sigma(j, V), F(j, V), Z(j, V) \xrightarrow{\text{Chiral Pert. Th.}} \Sigma, F, Z. \quad (3.11)$$

Fig. 15. The typical domains of application for two type of expansions indicated by lines of constant m_σ/m_π in the (κ, j) plane. The dashed curve corresponds to $m_\pi L = 1$ on a 10^4 lattice. The regions below (above) the dashed curve are the \mathcal{U} (\mathcal{V}) domains for $L = 10$ (from [64]).

There are two types of expansions, valid in different domains with a non-vanishing overlap (cf. fig. 15).

(\mathcal{U}) $m_\pi \lesssim 1/L$: This domain is characterized by very small symmetry breaking, where the symmetry is restored. The finite size effects are large here. The expansion is in powers of L^{-2} keeping the total magnetic energy

$$u_0 = \Sigma j L^4, \quad (3.12)$$

fixed. Thus j is treated as a quantity of the order $O(L^{-4})$. In \mathcal{U} the correlation length ξ_π grows as L^2 for $L \rightarrow \infty$.

(\mathcal{V}) $m_\pi \gtrsim 1/L$: In this region j is still small, although larger than in \mathcal{U} . Finite size effects are smaller than in \mathcal{U} . A typical range observed is $m_\sigma/m_\pi \gtrsim 5 - 10$. Here the symmetry is not restored. The expansion in powers of L^{-2} in that domain keeps fixed

$$v_0 = \Sigma j L^2 / F^2 = m_\pi^2 L^2. \quad (3.13)$$

For large u_0 the results of the expansion \mathcal{U} should smoothly go over into those of the expansion \mathcal{V} . There is an overlap of the regions of validity of both expansions around $m_\pi L \simeq 1$ [64]. In fig. 15 the dashed curve indicates where the \mathcal{U} and \mathcal{V} regions in the κ - j plane meet for $L = 10$.

We do not want to go into details of the various expansions. Just in order to catch the spirit of the approach let us give an example for one result of the \mathcal{U} -expansion.

$$\langle \varphi_x^0 \rangle_{V,j} = \frac{u}{jL^4} \frac{I_2(u)}{I_1(u)} + 2\rho_2 \frac{\Sigma^2}{F^4} j + O(L^{-6}), \quad (3.14)$$

where the second term is $O(L^{-4})$ and

$$\frac{u}{jL^4} = \Sigma \left[1 + \frac{3\beta_1}{2L^2 F^2} + O(L^{-4}) + O(L^{-6}) \right]. \quad (3.15)$$

The second term here is $O(L^{-2})$. The constant $\beta_1 = 0.14046$ depends on the lattice geometry, as does the constant in $\rho = 0.01523 + 0.0095 O(\ln L \Lambda_\Sigma)$. The terms $O(L^{-4})$ are small and involve higher orders in the chiral expansion.

Fig. 16. Example for the type of data obtained for $\langle \varphi_x^0 \rangle_{V,j}$ (from [64]). The solid curves correspond to a fit according (3.14) up to $O(L^{-2})$, the resulting value of the only parameter Σ is indicated by the full dot at $j = 0$.

Eq. (3.14) gives the functional form of the j and L dependence in terms of the thermodynamic quantities Σ and F . Fig. 16 gives an example of the type of data and fit quality obtained. The leading term in (3.14) provides the value of Σ . The non-leading term in principle can give F , but is statistically not sufficiently reliable. For this parameter one better uses the t -dependence of the Goldstone propagator.

The values $\Sigma(\kappa)$ obtained in this way prove to be very precise, as demonstrated in fig. 17. One should keep in mind, that these *are the thermodynamic values!* The fit to the scaling behaviour gives [64]

$$\Sigma^2 = 0.672(6)(-t)|\ln(-t)|^{\frac{1}{2}} \text{ and } \kappa_c = 0.3036(10). \quad (3.16)$$

Fig. 17. The values of Σ obtained from the fit of $j > 0$, finite volume data to the chiral perturbation expression; the curve shows the fit to the expected scaling behaviour (from [64]).

TABLE II
Results on various quantities of the $O(4)$ Φ^4 model as obtained with the action (1.3) in various studies.

κ	Σ	$\langle \bar{\varphi}^\alpha \rangle$	F	Z	m_σ	m_σ/F	Ref.
0.3130(7)	0.196(1)		0.199(5)	0.976(6)	0.50	2.517(65)	[102]
0.3101(5)	0.166(6)		0.168(5)	0.974(7)	0.40	2.380(69)	[102]
0.3077(3)	0.130(3)		0.132(3)	0.973(5)	0.30	2.280(58)	[102]
0.3058(2)	0.093(2)		0.094(2)	0.972(5)	0.20	2.129(46)	[102]
0.3046(1)	0.051(1)		0.052(1)	0.971(5)	0.10	1.941(34)	[102]
0.355	0.4036(9)	0.402	0.4109(13)	0.965(2)	1.09(10)	2.65(25)	[64]
0.330	0.3027(11)	0.301	0.3075(16)	0.969(3)	0.92(7)	2.99(24)	[64]
0.325	0.2769(12)	0.276	0.2807(19)	0.973(5)	0.81(2)	2.89(9)	[64]
0.310	0.1643(63)	0.163	0.1668(73)	0.97(1)	0.39(2)	2.34(22)	[64]
0.3075	0.132(13)	0.128	0.135(14)	0.96(1)	0.29(1)	2.15(30)	[64]
0.3100	0.15549(10)		0.1584(7)	0.964(7)	0.4073(7)	2.572(15)	[54]
0.3080	0.12827(6)		0.1301(3)	0.972(3)	0.3223(12)	2.477(14)	[54]
0.3060	0.09045(10)		0.0915(2)	0.977(3)	0.2072(7)	2.264(14)	[54]

In table II the values of Σ obtained by the discussed chiral perturbation expansion method [64] is compared with the original “brute force” ansatz (3.3) and one finds surprising agreement - although the new method definitely is of higher quality.

Let us summarize the different ways to determine the low energy parameters.

Determination of Σ : (a) from the $j > 0$ data with help of the discussed chiral perturbation expansion in j and L^{-2} ; (b) at $j=0$ from the distribution of the “local” mean magnetization $\langle |\bar{\varphi}^\alpha| \rangle$ defined in (3.3) – for a detailed discussion of this

constraint effective potential approach cf. [52, 55, 53, 54].

Determination of Z : from the Goldstone propagator (a) at $j > 0$ from chiral perturbation expansion formulae [64] and (b) at $j = 0$ using the field components transversal to the direction defined by the magnetization $\langle |\overline{\varphi}^\alpha| \rangle$.

Determination of m_σ : (a) from the component of the field parallel to the direction of $\overline{\varphi}^\alpha$ (for each configuration); (b) from the susceptibility

$$\chi = |\Lambda| (\langle |\overline{\varphi}^\alpha|^2 \rangle - \langle |\overline{\varphi}^\alpha| \rangle^2) , \quad (3.17)$$

which is in leading order proportional to $1/m_\sigma^2$. The latter method appears to work very efficiently [54].

Fig. 18. Comparison of results for the renormalized coupling for different values of the cutoff $\Lambda = 1/(am_\sigma)$ (from [113] in 1990).

In table II we compare the results derived over the years from various groups. One observes increasing quality of the numbers. Comparing the Monte Carlo results for the renormalized coupling at values $m_\sigma < 0.5$ with those of [100, 101, 102] one finds good agreement (within the statistical errors). This was also confirmed by further Monte Carlo results of other groups [87, 88, 7]. The resulting estimates for the upper bound on the renormalized coupling are shown in fig. 18 and fig. 19. One clearly notices the progress in the statistical accuracy.

If we assume that the cutoff (given in units of m_σ in the figure) should not be below ~ 2 then we read off an upper bound of $R \lesssim 2.6(3)$. With (2.3) this translates into $m_H \lesssim 670(80)$ GeV. This bound comes from the field theoretic properties of the Φ^4 model as a direct consequence of triviality and should not be mixed up with the so-called unitarity bound on the Higgs mass. The bound expresses the fact, that for this part of the standard model we cannot perform the continuum limit. Or, put differently, for a given Higgs mass there is a limited domain of validity of the regularized Φ^4 theory. If the Higgs mass comes out to be much smaller, e.g. of the order of 200 GeV, the bound allows a cutoff of the order of the Planck length. Up to the allowed cutoff we still can consider the theory a model with an effective

Fig. 19. Results for the renormalized coupling for different values of the cutoff $\Lambda = 1/(am_\sigma)$. The 4 points with larger error bars are from [102] and correspond to twice the error quoted, following their discussion of uncertainties. The upper group of points corresponds to a different action as will be discussed below (from [54] in 1992).

interaction. However, we conclude that the theory cannot be a truly fundamental one (we cannot remove the cutoff completely) and we therefore may expect constituent structure.

All these results have been obtained away from the critical point, therefore one does have contributions from non-leading operators. These corrections to scaling are regularization dependent and $O(a^2)$. The cutoff then represents new, possibly more fundamental physics which would replace the standard-model at higher energies. However, its influence is effective on all scales and manifests itself in the cutoff dependence of all observables. In describing the experiments through a lattice model, the higher in energy we go the stronger we expect such cutoff effects to be. More and more terms would have to be included in the effective action in order to explain experiments with sufficient accuracy. Within the scaling region one expects to find these dependencies to be only weak, but this knowledge is mainly based on rough estimates and there are only few explicit studies [7, 8, 70, 53, 54].

Value and shape of the bound depend on the adopted regularization scheme, i.e. on:

- The lattice geometry; an investigation of the scalar field theory on various types of lattices is required [7, 110, 112, 70]. Methods for comparing the results obtained by means of different regularization schemes are being developed [66, 102, 91]; they require calculations of high precision in a region of the coupling parameter space where the universal asymptotic scaling associated with the ("trivial") gaussian fixed point sets in.
- Additional terms in the action; an example is the introduction of a straight distance 2 coupling in order to remove the $O(p^4)$ dependence in the lattice perturbative propagator (Symanzik improvement).

- Other terms of $O(1/\Lambda^2)$ in the action; Heller et al. [72, 73, 74] have studied these effects in the $O(N)$ -model by systematically adding operators of increasing order in $1/\Lambda$, both, in continuum and on the lattice, in particular on an F_4 -lattice [110].
- Other regularization schemes: Recent work demonstrates the regularization dependence in the continuum $O(4)$ model with a higher derivative regulator [79, 78].

Comparing results from different actions obtained at finite cutoff is not straightforward, though. Different actions have different scaling violation properties. Choosing couplings such that the observed correlations lengths agree is not the only and not necessarily the best definition. Consider e.g. an effective action for block variables (which usually is more complicated). Comparing the results of the original and the block action at a point in their respective coupling constant spaces where the dimensionless correlation lengths agree, the block action will definitely have better continuum properties, it has less corrections to the leading scaling behaviour. It is “closer to the continuum limit”.

In an asymptotically free theory that issue can be resolved by comparing the behaviour of the β -function in the weak coupling region [61, 100, 66]. In our case in principle we can rely on renormalized perturbation theory. In fact the proportionality constant C in the two-loop expansion for the renormalized mass in (3.1) is regularization scheme dependent. We therefore add a subscript s denoting the regularization scheme (lattice action or geometry). Asymptotically, at small enough small λ_r , $a_s/a_{s'} = C_s/C_{s'}$ can be determined by lattice perturbation theory.

For a comparison of different effective theories at finite cutoff and not too small λ_r we can no longer rely on that approach. It would be appropriate to choose another physical observable \mathcal{O} , that may serve as a means to measure the distance from the continuum limit independently. Comparing results due to different actions S_s (where the index distinguishes between the different actions and regularization schemes) at the same values of \mathcal{O} then provides an estimate for the regularization dependence. This observable could be for example a $\pi\pi$ -scattering cross-section, the σ -decay width or the violation of euclidean rotational invariance of some quantities [102, 8, 70, 54, 93]. Different operators \mathcal{O} will usually have different cutoff dependence and their choice needs further motivation: There is no “best” observable. Quantities like the ratio R should be considered versus such a “distance” \mathcal{O} to the continuum limit. Of course we could still use the inverse correlation length $m_{\text{phys}}a_s$, but in order to compare different schemes we have to rescale a_s at each point such that \mathcal{O} agrees.

In a Monte Carlo study of the 1-component Φ^4 model [93] the violation of euclidean rotational invariance (in real space and in momentum space) of the Higgs-propagator was used as measure for the “distance to the continuum limit”. Four kinds of lattice actions, respectively lattice geometries, were considered.

\mathcal{C} : The standard action on the hypercubic lattice (1.2).

\mathcal{C}' : An action including diagonal nearest neighbour terms with the same coupling [7].

\mathcal{F}_4 : The nearest neighbour action on an F_4 -lattice [8, 9]. It’s embedding into a hypercubic lattice may be imagined by removing all odd sites of the grid. The

symmetries for this case forbid terms like $\sum_{\mu} p_{\mu}^4$ in the inverse momentum space propagator and guarantee Lorentz-invariance to a higher order in the momentum cutoff $O(\Lambda^{-4})$ than the first two hypercubic lattice schemes which had violating terms $O(\Lambda^{-2})$.

S : The Symanzik improved action which includes anti-ferromagnetic couplings to the next-to-nearest neighbours along the 4 euclidean axis-directions. These additional terms are incorporated in order to remove the undesired $O(\Lambda^{-2})$ contributions. The remaining corrections of $O(\Lambda^{-4})$ in the lattice dispersion relation guarantee tree-level improvement [134].

All four lattices may be embedded into the regular hypercubic one.

Fig. 20. Fig. from [93], showing the amount of rotational symmetry in the inverse boson propagator in momentum space, determined for 4 different actions.

Fig. 20 compares the rotational invariance properties for the boson propagator in momentum space. The deviation from the exact continuum symmetry may be quantified by considering the coefficients in an expansion in spherical harmonics. Fig. 21 exhibits the final results for $R = m_{\sigma}/F$ (proportional to the square root of the renormalized coupling) as functions of a measure for the deviation from rotational symmetry. As discussed above, this may be a more appropriate measure than the correlation length itself. One finds a sizable difference, about 30-40%, between the values for the actions **C** and **C'** (which violate rotational invariance to a larger extent) on one hand and **F₄** and **S** on the other (which have no $O(p^4)$ violation in the tree-level propagator).

Fig. 21. The ratio (2.3) vs. a measure of rotational invariance for the one-component model; the curves are fits to the asymptotic behaviour; the left-hand part give the results on an extended scale. The symbols used denote the different action (C : bars, C' : squares, F_4 : triangles, S : asterisks) (fig. from [93]).

In the results for the $O(4)$ model for F_4 [8] and S [54] the authors estimated the regularization dependence by comparing the results at given value of another measure of rotational symmetry, derived from a perturbation expansion of the Goldstone-Goldstone scattering cross-section. There the difference between F_4 , S compared to C was smaller than that observed in [93], of the order of 10-20 % for 1-10% violation of rotational symmetry. Although this variation could be due to the study of different models (one component vs. four component fields) it may also indicate a strong dependence on the choice of measure for rotational invariance. Maybe systematic studies of higher order terms, like those initiated recently [74, 72, 73, 79, 78] are helpful to clarify this issue.

Let us conclude this chapter with a summary of the Monte Carlo results for the $O(4)$ Φ^4 model.

- The observed scaling behaviour is consistent with the triviality conjecture.
- One clearly identifies Goldstone bosons and the massive Higgs mode.
- One finds good agreement with analytically derived results in regions, where the comparison is possible ($am_H < 0.5$).
- Finite size scaling works.
- Chiral perturbation theory provides an excellent description of $j > 0$ finite volume results and allows a reliable extrapolation to the thermodynamic situation of spontaneous symmetry breaking.
- Allowing for a cutoff $> 2m_H$ (or “continuum-like behaviour” up to a few percent) one obtains an upper bound for the renormalized coupling, that translates (using the experimental values for the gauge coupling and the W -mass) into the bound on the Higgs mass [71],

$$m_H < 710(60)\text{GeV}. \quad (3.18)$$

- Some (relatively weak) regularization dependence of this bound (and other quantities) has been observed.
- Further work includes fermions (Yukawa models), but no drastic change of the bound has been found.

The recent review of Heller [71] summarizes the situation and gives further relevant references.

4. SCATTERING: PHASE SHIFTS AND RESONANCES

Most observables that have been considered in lattice calculations so far are *masses* (from propagators) and *coupling constants*. Most experimental measurements in high energy physics, however, lead to cross sections and their analyses to scattering phase shifts. Indeed, resonances are described by the slope and position of the values of the phase shift passing through $\pi/2$ and the width is a quantity derived under certain additional assumptions (like the Breit-Wigner shape). In fact, considering the $O(4)$ Φ^4 model we are in a situation, where the Higgs boson is a resonance (coupling to Goldstone states) and, strictly speaking, no asymptotic state of the theory. For the determination of the Higgs mass it is therefore not sufficient to just determine the single particle propagator over larger and larger distances. In that limit one will only learn about the lowest lying energy level in that channel, which is not the Higgs mass but a 2-particle threshold.

In finite systems the energy spectrum is discrete and may be related to the phase shifts in the infinite volume system [96, 97, 103, 99, 98]. The leading volume dependence is connected to the scattering lengths and early calculations in the 4D Ising model determined the s-wave scattering length [108, 39]. Meanwhile there are several studies:

- In a pioneering work Lüscher and Wolff obtained phase shifts in the 2D $O(3)$ nonlinear σ -model [103]. There the result is known analytically from conformal field theory and one found agreement with the non-perturbative calculations.
- Below I discuss another 2D study [45, 46, 44] with the aim to determine phase shifts in a resonating situation and to find the resonance parameters in a non-perturbative way.
- Fiebig et al. [34, 35] investigate the 3D QED and determined phase shifts for the scattering of mesonic bound states (in the quenched situation, i.e. without dynamical fermions in the vacuum).
- In the 4D $O(4)$ Φ^4 model there have been studies in the symmetric phase [114] and in the broken phase with an additional external symmetry breaking field [148, 149, 139]. The latter model is a test case for resonating phase shifts as well, since one has a situation with light particles (the Goldstone bosons have non-zero mass due to the external field) and one heavy resonance (the Higgs particle decays into the Goldstone states and is no asymptotic state of the theory).

Only the efficient algorithms available for bosonic systems allow the high precision that is necessary to determine the energy levels and phase shifts, as discussed below. For this reason the scalar field theories are the leaders in that approach – the reason to discuss approach and result in this last section of this review. Also, in that process a lot can be learned on the representation of physical states on the lattice.

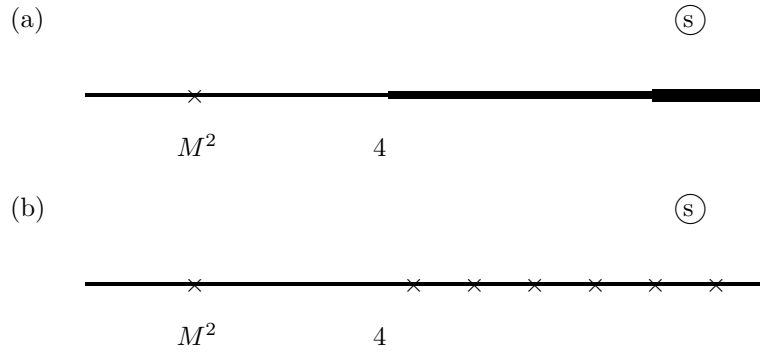


Fig. 22. The spectral density in the $s = W^2$ -plane; (a) infinite volume, (b) finite volume.

4.1. Energy Eigenspectrum of Finite Systems

Consider the propagation of a state $|N\rangle$ in a channel with 1-particle (mass M) and 2-particle states (mass $m = 1$, i.e. we choose the light state as the mass unit for simplicity of notation, where not stated otherwise). In infinite volume the analytical structure of the propagator in the relativistic variable s is as shown in fig. 22(a), with an elastic cut starting at $4m^2 \equiv 4$, higher inelastic thresholds and (for $M < 2m$) a bound state below the elastic threshold. The dispersion relation representation gives

$$T(s) = \text{pole} + \frac{1}{\pi} \int_4^\infty ds' \frac{\rho(s')}{(s' - s)} \quad (4.1)$$

or, Fourier transformed to euclidean time t ,

$$G(t) = c_0 e^{-Mt} + \frac{1}{\pi} \int_4^\infty dW' e^{-W't} \rho(W') \quad (4.2)$$

where W denotes the energy and ρ is the spectral density. If the single particle state is above threshold it describes a resonance and is no longer part of the discrete spectrum and no longer an asymptotic state.

In finite volume the continuous spectrum is replaced by a discrete set (cf. fig. 22(b)),

$$G(t) = c_0 e^{-Mt} + \sum_i c_i e^{-W_i t}, \quad (4.3)$$

with the eigenspectrum $\{W_i\}$. A possible resonance is represented by the form of the discrete spectrum and not by a single energy level like a bound state.

How can we determine the eigenspectrum in realistic lattice calculations? The answer is given by standard methods of quantum mechanics. One has to find a (sufficiently) complete set of operators N_n with the correct quantum numbers (symmetry properties) of that channel. Each $N_n(t)$, $n = 1, 2, \dots$ is defined on a single time

slice, and t denotes the separation of the time slices. In the Monte Carlo simulation one then measures the connected correlator,

$$C_{nm}(t) = \langle N_n^*(0)N_m(t) \rangle_c \equiv \langle N_n^*(0)N_m(t) \rangle - \langle N_n^* \rangle \langle N_m \rangle . \quad (4.4)$$

The transfer matrix formalism (see e.g. [77]) yields the spectral decomposition

$$C_{nm}(t) = \sum_l \langle N_n^* | l \rangle e^{-W_l t} \langle l | N_m \rangle_c \quad (4.5)$$

$$= \sum_l v_n^{(l)*} v_m^{(l)} e^{-W_l t} . \quad (4.6)$$

For simplicity we assume non-degenerate W_l , ordered increasingly. The amplitudes $v_n^{(l)} = \langle l | N_n \rangle$ are the projections of the states $|N_n\rangle$ (generated by the operators N_n out of the vacuum) on the energy eigenstates $\langle l |$ of the scattering problem.

In actual calculations one has to truncate the correlation matrix, since one can consider only a finite number r of operators. The generalized eigenvalue problem

$$C(t) \zeta^{(k)}(t) = \lambda^{(k)}(t, t_0) C(t_0) \zeta^{(k)}(t) , \quad k = 1, 2, \dots, r . \quad (4.7)$$

allows one to find the energy eigenvalues W_l efficiently even for comparatively small values of t . In (4.7) we assume $t_0 < t$, e.g. $t_0 = 1$. We require the N_n , $n = 1, 2, \dots, r$ to be linearly independent, thus $C(t_0)$ is regular and the generalized eigenvalue problem is well defined. Indeed, it may be transformed to a standard eigenvalue problem for the matrix

$$C^{-\frac{1}{2}}(t_0) C(t) C^{-\frac{1}{2}}(t_0) , \quad (4.8)$$

with identical eigenvalues $\lambda^{(k)}(t, t_0)$ and eigenvectors $\mathbf{u}^{(k)}(t) = C^{\frac{1}{2}}(t_0) \zeta^{(k)}(t)$. The solution for the eigenvalues is

$$\lambda^{(k)}(t, t_0) = e^{-(t-t_0)W_k} . \quad (4.9)$$

Some approximations have to be done in the numerical calculations, among them the restriction to a finite set of lattice operators and therefore to a finite set of eigenvalues. However, as has been pointed out in [103], the correction due to the truncation is of $O(\exp[-(t-t_0)W_{r+1}])$ by a perturbation calculation. The range of t -values is dictated by statistical errors of the values of the correlation function and is usually between 1 and 8.

4.2. Spectrum and Phase Shifts

Consider quantum mechanics in a $(d-1)$ -dimensional spatial box, with periodic (torus) boundary conditions with cubic symmetry. Assume that the interaction region is localized and smaller than the extension of the box. Solving the static Schrödinger equation outside the interaction region ($V = 0$, i.e. the Helmholtz equation) and expanding the solution into cubic ($SO(d-1, \mathbb{Z})$) spherical harmonics one finds a relation between the discrete values of the momenta and the phase shift

at these points [97, 103, 99]. As a simple example we consider the scalar A_1^+ sector and neglect higher angular momenta (> 3). We find

$$\exp(2i\delta_0(k)) = \frac{m_{00}(k) + i}{m_{00}(k) - i}, \quad (4.10)$$

$$m_{00}(k) = \mathcal{Z}_{00}(1; q^2)/q\pi^{\frac{3}{2}} \quad \text{where} \quad q = \frac{kL}{2\pi}, \quad (4.11)$$

i.e. $m_{00}(k) = \cot \delta_0(k)$, the usual K -matrix. The function \mathcal{Z}_{00} is a generalized zeta-function, and one has

$$\begin{aligned} m_{00}(k) &= \cot q\pi && \text{for } d=2, \\ &= \frac{1}{4\pi^2 q} \sum_{\vec{n} \in \mathbb{Z}^3} \frac{1}{\vec{n}^2 - q^2} && \text{for } d=4. \end{aligned} \quad (4.12)$$

This gives a relation

$$\delta(k_n) = n\pi - \Phi(k_n) \quad (4.13)$$

between the quantized values of k and the phase shift. For $d = 4$ the functional form of $\Phi(k)$ is determined numerically (cf. [149]). For $d = 2$ one has the simple form $\Phi(k_n) = k_n L/2$ and thus

$$2\delta(k_n) + k_n L = 2n\pi \quad (n \in \mathbb{Z}), \quad (4.14)$$

and this quantization condition may be easily visualized for the cases without and with interaction (fig. 23). Because of the periodic b.c. of the wave functions one has $\Psi(0) = \Psi(L)$, $\Psi'(0) = \Psi'(L)$. Due to the (localized) interaction a non-zero phase shift affects the quantization of the momenta.

Fig. 23. The quantization in $d=1$ (a) without and (b) with interaction phase shift.

These arguments and the equation (4.12) may be applied to a quantum field theory problem under the following restrictions and assumptions.

- The interaction region is localized $< L$ and, in particular, the size of the single particle states is smaller than the lattice: $1/m \ll L$. This is due to that one wants a pair of two free particles as asymptotic states.
- The polarization effects are controllable. Of course there will be interaction, e.g. self interaction of the light particles around the torus world. In fact this is perturbatively the leading contribution. This effect can be understood and accounted for.

- On is confined to the elastic regime $4 < s < 9$ (for a 3-particle inelastic threshold, or 16 for a 4-particle threshold, depending on the quantum number of the channel).
- One understands the lattice artifacts (they are $O(a^2)$). This is because we work close to but never at the phase transition. These terms are due to the grained structure of the lattice and leading contributions may be studied already in the non-interacting gaussian model.

For the determination of the energy spectrum one should consider correlation functions of a sufficiently large number of observables with the correct quantum numbers, capable to represent the eigenspace of scattering states [103].

To summarize, for a given set of couplings the determination of the phase shifts in the scattering sector (at total momentum zero) consists of the following steps.

1. For given lattice size L determine the single particle state; check for polarization effects and get the mass m .
2. Determine the correlation matrix $C(t)$ for various values of t , solve the eigenvalue problem for this matrix, and obtain the spectrum from the exponential decay (4.9). The dimension r of C cannot be chosen too large, because then the inversion becomes numerically unstable. We denote the energy eigenvalues by $W_n(L)$.
3. From the values $W_n(L)$ one finds k_n with help of the dispersion relation

$$W_n = 2\sqrt{m^2 + k_n^2}. \quad (4.15)$$

This uses the fact that the 2-particle energy is the sum of the (back to back) outgoing single particle energies.

4. From the values k_n one obtains $\delta(k_n)$ from (4.13).

For each lattice size L one obtains in this way several (typically the lowest 1–4) energy eigenvalues and thus pairs $k_n, \delta(k_n)$. The procedure is then repeated for other lattice sizes. Eventually one gets more and more values k and δ , filling the domain $0 < k < \sqrt{5/4}$ (or $\sqrt{3}$ if the 4-particle threshold is the first inelastic one). In fig. 24 the spectrum of free 2-particle states (vanishing phase shift) for the 4D system is shown.

4.3. Models and Results

Here I want to discuss two studies of scalar models and their results, concentrating on common features.

4.3.1. 2D Resonance Model

The authors [45, 46, 44] study a model, which describes two light particles φ that couple to a heavier particle η giving rise to resonating behaviour. For this one couples two Ising fields through a 3-point term,

$$S = S_{\text{Ising}}(\varphi, \kappa_\varphi) + S_{\text{Ising}}(\eta, \kappa_\eta) + \frac{g}{2} \sum_{x \in \Lambda, \mu=1,2} \eta_x \varphi_x (\varphi_{x-\hat{\mu}} + \varphi_{x+\hat{\mu}}). \quad (4.16)$$

The values of the fields are restricted to $\{+1, -1\}$ and S_{Ising} denotes the usual action of the Ising model. The 3-point term is introduced in a nonlocal manner,

Fig. 24. The free 2-particle energy spectrum ($\delta = 0$) according to (4.13); the density increases with the volume (from [148]).

because $\varphi_x^2 \equiv 1$. The system is studied in the symmetric phase with regard to both nearest-neighbour coupling κ_φ and κ_η .

The case $g = 0$ corresponds to the situation of two independent Ising models, each with a 2nd order phase transition at $\kappa_c = \frac{1}{2} \ln(1 + \sqrt{2}) \simeq 0.44068$. In the scaling limit the model describes an interacting boson with mass $m = -\log(\tanh \kappa) - 2\kappa$ [77]. Reformulating the Ising model at the phase transition as a theory of non-interacting fermions, it was shown that the scattering matrix assumes the value -1 independent of the momentum [119].

In the coupled case ($g > 0$), if we identify η and φ with particle states, the term proportional to g gives rise to transitions like $\eta \rightarrow \varphi\varphi$ rendering η a resonance in the $\varphi\varphi$ channel, when kinematically allowed. The phase diagram of this model has interesting structure with limiting cases including random external fields and random bond models. Its structure is discussed in more detail in [46].

The values of the couplings $\kappa_\varphi, \kappa_\eta$ are adjusted such that $m_\varphi = 0.19$ and $m_\eta = 0.50$. The system is studied for the case of two independent Ising models $g = 0$ as well as for the values $g=0.02, 0.04$. The lattice sizes $L \times T$ considered were in the range $L = 12 \dots 60$ and $T = 60 \dots 100$. Cluster updating was used, with typically 200 K measurements per point. In the 2-particle channel 4–6 operators N_n were considered and 2–5 lowest eigenvalues determined from diagonalizing the correlation function at distances $\Delta t = 2 \dots 8$.

4.3.2. $O(4)$ Φ^4 Model

Zimmermann et al. [148, 149, 139] study the $\lambda \rightarrow \infty$ limit of the $O(4)$ model, i.e. the nonlinear σ -model, with a small external field. As discussed, this is a theory with three degenerate light pions $\vec{\pi}$ (would-be-Goldstone bosons) and a heavy σ (the Higgs boson).

The bare coupling parameters κ and j were adjusted to have renormalized masses

$m_\pi = 0.23$ and $m_\sigma = 0.70$. The system was simulated with the cluster algorithm on lattices of size $L^3 \times T$ with $L = 12 \dots 32$ and $T = 32 \dots 40$ (40-50 K measurements per point). The authors considered 6 operators in the 2-particle channel and determined typically 2-5 lowest energy eigenvalues from the correlator at distances $\Delta t = 2 \dots 8$.

4.3.3. Single Particle States

For the determination of the energy spectrum a precise knowledge of the single particle mass and related finite size effects is important. The operator of a φ state with momentum

$$p_\nu = 2\pi\nu/L, \quad \nu = -L/2 + 1, \dots, L/2 \quad (4.17)$$

may be represented through

$$\varphi(p_\nu, t) = \frac{1}{L^{d-1}} \sum_x \varphi(x, t) \exp(ip_\nu x). \quad (4.18)$$

Its connected correlation function over temporal distance t decays exponentially $\propto \exp(-E_\nu|t|)$ defining the single particle energy E_ν ; in particular we have $E_{\nu=0} = m_\varphi$.

The observed mass, as compared to the “real” mass at vanishing lattice spacing and infinite volume, incorporates contributions from polarization due to self interaction around the torus (decreasing exponentially with L) and lattice artifacts due to the finite ultra-violet cutoff (polynomial in the lattice constant a).

Fig. 25. Results (E_ν, p_ν) as obtained from the analysis of the single particle propagator in the 2D Ising model ($g = 0$, $L = 50$, from [46]). The dashed curve represents the continuum d.r. (4.19) and the full curve the lattice d.r. (4.20).

Fig. 25 is a plot of E_ν vs. p_ν , obtained for the pure Ising model ($g = 0$) and $L = 50$. Comparing the values (E_ν, p_ν) with the continuum spectral relation ,

$$E_\nu = \sqrt{m^2 + p_\nu^2} \quad (4.19)$$

one observes deviations $O((ap)^2)$, as expected [103]. Using the dispersion relation for the lattice propagator of a gaussian particle with mass m ,

$$E_\nu = \text{arcosh}(1 - \cos p_\nu + \cosh m) , \quad (4.20)$$

one finds excellent agreement with the measured values. Thus this particular single particle state shows little deviation from the free lattice form. These results for the 2D Ising model holds for the situations $g \neq 0$ as well and was confirmed in the 4D study [148, 149, 139], too.

Let us, for the moment, stay with the 2D Ising model. It may be considered the limit of a Φ^4 theory with infinite bare 4-point coupling λ . We are in the symmetric phase, thus we expect the leading interaction to be due to an effective 4-point term. The finiteness of the spatial volume allows self-interaction with one particle running around the torus. This leads to a finite volume correction to the particle mass proportional to $\lambda_r e^{-mL}/\sqrt{L}$. In the 2D model excellent agreement with this behaviour was observed. This mass shift on finite lattices has also been confirmed in Monte Carlo simulations of the Ising model in 4 dimensions [108].

4.3.4. Scattering Sector

In the 2-particle channel one considers operators with total momentum zero and quantum numbers of the η , a set as complete as possible. These operators may be constructed from the $p = 0$ single η -operator,

$$N_1(t) \equiv \eta(p = 0, t) = \frac{1}{L^{d-1}} \sum_x \eta(x, t) \quad (4.21)$$

as well as from the combination of two φ -operators with opposite momentum,

$$N_n(t) = \sum_p f_n(p) \varphi(-p, t) \varphi(p, t) , \quad (4.22)$$

$$\varphi(p, t) = \frac{1}{L^{d-1}} \sum_x e^{2i\pi(x \cdot p)/L} \varphi(x, t) , \quad (4.23)$$

where p and x have $d - 1$ (integer valued) components. The wave function in momentum space $f_n(p)$ has been chosen in various ways.

- Plane waves would be the eigenstates for the non-interacting case. This corresponds to choosing all integer values of $|p|^2$,

$$\begin{aligned} f_n(p) &= \delta(n, |p|) \quad \text{for } d = 2 , \\ f_n(p) &= \delta(n, |p|^2) \quad \text{for } d = 4 . \end{aligned} \quad (4.24)$$

- However, one could also choose special forms like the periodic singular solutions of the Helmholtz equation

$$f_n(p) = \frac{1}{p^2 - q_n^2} \quad (4.25)$$

as has been tried in [149].

The question here is which choice gives the best representation of the scattering eigenstates. Any “complete” set would do in principle, but in practice one is limited to a small number of operators and thus there may be “bad” and “better” choices. In the calculations discussed here no clear priority for one of the discussed forms was found. Both worked equally good; thus one favours the simpler form (4.24).

These operators and products thereof are now measured for each configuration and the resulting correlation function (4.4) is computed for various values of t , diagonalized and the energy spectrum determined from the exponential decay (4.9).

Fig. 26. The lowest energy levels for (a) the non-interacting gaussian model and (b) the Ising model; the decoupled η -state is also shown. The full lines denote curves due to phase shifts (a) $\delta = 0$ and (b) $\delta = -\frac{\pi}{2}$ (fig. from [46]).

Fig. 27. The phase shift obtained for the Ising model from the energy spectrum in fig. 26 (fig. from [46]).

In fig. 26 we compare the results for the energy levels for the 2D Ising with those for the free, non-interacting case. We find that the lowest level moves from the threshold (in the free case) to higher values in the Ising situation. In the figure we

also plot the results of the (decoupled) single η state at $m_\eta = 0.5$. The level crossing therefore is fictitious and does not really occur, since the $\varphi\varphi$ channel is decoupled from the η -channel ($g = 0$). We note that we have only a few energy eigenstates between the elastic threshold (at 0.38) and the inelastic threshold (at 0.76).

The critical 2D Ising model has an S -matrix equal to -1 and we therefore expect a phase shift $\delta_{\text{Ising}} = -\frac{\pi}{2} \pmod{\pi}$ in the scaling regime. Fig. 27 shows the results for the phase shift $\delta(k)$ determined from the data for the Ising model (fig. 26(b)) as a function of the dimensionless momentum k/m_φ .

Figs. 28 exhibit results of the 2D resonance model in the coupled situation, for $g \neq 0$. For most of the points the errors are smaller than the symbols, typically 0.5% of the energy value. The degeneracies in the energy spectrum have now disappeared, resulting in avoided level crossing with a gap that grows with g .

Fig. 28. Left: The measured energy levels for the $\varphi\varphi$ channel for the coupling constant values $g = 0.02$, vs. the spatial lattice extension L . The full curves show the theoretical expectations for the values from the phase shift as discussed in the text. The dashed lines indicate the 2- and the 4-particle thresholds. Right: The phase shift as determined from the energy levels (fig. from [46]).

One should keep in mind that points at neighbored values of k may come from quite different values of L and different branches of energy levels. In order to emphasize this situation corresponding symbols denote the energy values on one branch, i.e. for one value of n . Each branch, from small to large L contributes to the whole range of k values; it starts at larger values of W (or k) with a phase shift close to $\pi/2$, passes through the resonance value at the plateau and approaches $-\pi/2$ towards smaller k . The overall consistent behaviour is impressive. The high energy values, corresponding to large k may feel the lattice cutoff effects $O(a^2)$ as well as possible misrepresentation of the energy eigenstates by the considered operators. Within the accuracy of the data none of these effects seems to be a problem.

The observed overall behaviour has a simple interpretation: A resonating phase shift superimposes the background Ising phase shift. The resonance parameters may

be determined from the phase shift like from experimental data, e.g. by a K -matrix fit or an effective range approximation.

Fig. 29. The energy levels in both s-wave channels of the 4D $O(4)$ model for a particular choice of couplings ($m_\pi = 0.295, m_\sigma = 0.906$); the dashed curves denote results due to renormalized perturbation theory (from [148]).

Fig. 30. The isospin 0 s-wave phase shift with the Higgs resonance determined from the energy spectrum in a non-perturbative Monte Carlo simulation (from [148]).

Similar results were obtained in the study of the 4D $O(4)$ model. In 4 dimensions the numerical task is much more demanding and therefore one could not study as broad a range of lattice sizes as in the 2D case. However, the region of the first

avoided level crossing could be reached, as demonstrated in fig. 29. Fig. 30 gives the isospin 0 s-wave phase shift; this is the channel with the Higgs resonance.

4.4. What Can We Learn?

4.4.1. Comparison to Perturbation Theory

The value of the partial width agrees with the Born term approximation using the value of the renormalized 3-point coupling [148, 139]. This implies that the situation is indeed described by an effective Lagrangian with tree-level expansion. However, the effective couplings have to be determined from the non-perturbative Monte Carlo calculation.

4.4.2. Representation of Operators in the Scattering Channel

In realistic situations we have to consider scattering between boundstates: In QCD the asymptotic states are bound states of the original quark fields, indeed a very demanding situation. One of the results of the purely bosonic scattering studies presented above concerns the quality of the representation of states through the lattice operators $N_n(t)$.

If the set of lattice operators $N_n(t)$ is complete, we may relate the eigenvectors of the diagonalization (4.8) to the physical eigenvectors $\zeta^{(k)}(t) \propto \mathbf{v}^{(l)}$ [45]. Let us express the original approximation (4.5) to $C(t)$ in terms of these eigenvectors,

$$C_{nm}(t) = \sum_{l=1}^r \zeta_n^{(l)*} \zeta_m^{(l)} |\mathbf{v}^{(l)}|^2 e^{-tW_l}, \quad n, m = 1, 2 \dots r. \quad (4.26)$$

In particular consider the diagonal element

$$C_{nn}(t) = \sum_{l=1}^r |\zeta_n^{(l)}|^2 |\mathbf{v}^{(l)}|^2 e^{-tW_l}. \quad (4.27)$$

For a continuous energy spectrum,

$$C_{nn}(t) = \int dW \rho_n(W) e^{-tW}, \quad (4.28)$$

and we identify $|\zeta_n^{(l)}|^2 |\mathbf{v}^{(l)}|^2 \propto \rho_n(W_l)$, the spectral density of the correlation function of operator N_n . We therefore find that $|\zeta_n^{(l)}|^2$ indicates the relative weight of the contribution of operator N_n to the energy eigenstate $|l\rangle$.

Fig. 31 shows the relative weights $|\zeta_n^{(l)}|^2$ for $l = 1, 2, 3$ and $n = 1, 2, 3$ for the 2D resonance model (case $g=0.04$). From the figure it can be seen, that the most important contributions to an eigenstate come from lattice operators that have similar eigenenergies in their eigensystem. Compare the energy spectrum of fig.s 26 and 28 with fig. 31. For small L the lowest energy state W_1 is close to the resonance energy. There the state is completely dominated by the η -operator N_1 (circles in fig. 28), which describes an η -particle at rest. For increasing L , W_1 decreases and approaches the 2-particle threshold. This manifests itself in a drastic decline of the contribution of N_1 , accompanied by an increase of the amplitudes for two φ -particles at rest

Fig. 31. Contributions of the operators N_1, N_2 and N_3 (circles, triangles, squares) to the energy eigenstates (a) $|1\rangle$, (b) $|2\rangle$ and (c) $|3\rangle$, displayed as a function of the lattice size L (fig. from [46]).

(operator N_2 , triangles) and with relative unit-momentum (operator N_3 , squares). For lattice size larger than 20, the energy W_1 is already too far below the resonance energy so that the energetically higher η at rest cannot contribute much to $|1\rangle$.

In this way we may discuss the other levels as well. E.g. the contribution of the η -operator N_1 (circles) to the second lowest state $|2\rangle$ assumes peak values where it crosses the resonance energy plateau.

Also, with this consideration we can identify misrepresentation of energy eigenstates in terms of the considered operators. At higher energies one observes a shift of the weight factors $|\zeta_n^{(l)}|^2$ towards higher operators N_n . If one has a situation, where the center of weight lies outside the scope of operators considered, more operators should be included for a good representation of that state [45]. The study of the representation of scattering states by the operators entering the correlation functions therefore sheds light on the problem of constructing good approximations for the energy eigenstates and it allows to control unwanted truncation effects.

4.4.3. Lattice Artifacts

In [44] the calculations for the Ising model were repeated for different coupling, corresponding to coarser lattice spacing. One found a stronger deviation from the expected phase shift at $am_\varphi = 0.5$ than at $am_\varphi = 0.19$, compatible with the expected corrections $O(a^2)$. However, as mentioned earlier, the d.r. (4.15) gives the total energy of the asymptotic 2-particle state which (under the assumption of localized interaction region) is just twice the energy of the outgoing particles. Now the $O(a^2)$ corrections of the single particle d.r. have been nicely described by replacing the continuum d.r. by the lattice relation (4.29). If one replaces (4.15) by the corresponding lattice expression,

$$W_n = 2 \operatorname{arcosh}(1 - \cos k_n + \cosh m), \quad (4.29)$$

the data for W_n now produce slightly different values of k_n and δ , in much better agreement with a constant value of $-\pi/2$. One concludes, that the leading $O(a^2)$ corrections can be expressed by replacing the continuum d.r. by the lattice relation. This observation was confirmed in the study of the 4D model [148].

In summary, it seems that Lüscher's method to determine phase shifts from the volume dependence of the discrete energy spectrum works nicely, also for resonances. There are problems, where some of the restrictions cannot be met. In cases where more than one channel has non-vanishing phase shifts the determining equation involves matrices and the identification becomes problematic. Most likely one needs further continuity arguments like those used in the phase shift analyses of experiments.

CONCLUSION

During the last decade computer simulation have become an important tool in QFT. Within the realm of purely bosonic field theory efficient stochastic algorithms have been developed, that allow high precision results. Almost always, however, it is insufficient to just let the programs run and wait long enough until the answer stabilizes. Finite size and relaxation problems are persistent. In certain limits we may have an idea of the structure of an underlying (possibly: effective) field theory that will have unknown parameters and a limited domain of validity. In this way different effective models may describe different limiting cases of the microscopic theory. The nonperturbative Monte Carlo calculations can provide the unknown values of the parameters in *ab initio* calculations. This has made the results based on a finite volume theory (like finite size scaling from renormalization group, chiral perturbation theory, or the finite volume dependence in the situation of phase shifts, to mention the examples discussed here) the most reliable ones.

The good agreement of Monte Carlo results with analytical expectations has opened the way for more sophisticated applications like using the Monte Carlo approach as an "experimental" test laboratory for quantum field theory models. Obviously one cannot hope to prove something (maybe one can disprove some ideas) but one can hope to identify relatively quickly promising or most-likely-bad theories. An example for this approach is the study of Yukawa-models and chiral fermions (cf. the review in [27]). The more conservative reason for Monte Carlo studies, and still the main motivation, is the possibility to determine numbers in this direct, non-perturbative quantization scheme, that are up to now not at all obtainable with other methods.

REFERENCES

- [1] M. Aizenman, Phys. Rev. Lett. **47** (1981) 1.
- [2] M. Aizenman, Commun. Math. Phys. **86** (1982) 1.
- [3] M. Aizenman and R. Graham, Nucl. Phys. B **225** [FS9] (1983) 261.
- [4] M. N. Barber, in *Phase Transitions and Critical Phenomena*, edited by C. Domb and J. Lebowitz, volume VIII, Academic Press, New York, 1983.
- [5] B. Berg and T. Neuhaus, Phys. Lett. B **267** (1991) 249.
- [6] B. Berg and T. Neuhaus, Phys. Rev. Lett. **68** (1992) 9.
- [7] G. Bhanot and K. Bitar, Phys. Rev. Lett. **61** (1988) 798.

- [8] G. Bhanot, K. Bitar, U. M. Heller, and H. Neuberger, Nucl. Phys. B **343** (1990) 467.
- [9] G. Bhanot, K. Bitar, U. M. Heller, and H. Neuberger, Nucl. Phys. B **353** (1991) 551.
- [10] K. Binder, Finite size effects at phase transitions, in *Computational Methods in Field Theory Lecture Notes in Physics 409*, edited by H. Gausterer and C. B. Lang, page 59, Springer-Verlag, Berlin, Heidelberg, 1992.
- [11] H. W. J. Bloete and R. H. Swendsen, Phys. Rev. B **22** (1980) 4481.
- [12] K. C. Bowler et al., Phys. Lett. B **179** (1986) 375.
- [13] E. Brézin, J. Physique **43** (1982) 15.
- [14] E. Brézin, J. C. Le Guillou, and J. Zinn-Justin, Field theoretical approach to critical phenomena, in *Phase Transitions and Critical Phenomena*, edited by C. Domb and M. S. Green, volume VI, page 127, Academic Press: New York, 1976), 1976.
- [15] D. Brydges, J. Fröhlich, and A. D. Sokal, Commun. Math. Phys. **91** (1983) 141.
- [16] D. C. Brydges, J. Fröhlich, and T. Spencer, Commun. Math. Phys. **83** (1982) 123.
- [17] T. W. Burkhardt and J. M. J. van Leeuwen, Progress and problems in real-space renormalization, in *Real-space Renormalization*, edited by T. W. Burkhardt and J. M. J. van Leeuwen, page 1, Springer-Verlag Heidelberg, 1982.
- [18] T. W. Burkhardt and J. M. J. van Leeuwen, editors, *Real-space Renormalization*, Springer-Verlag Heidelberg, 1982.
- [19] N. Cabibbo, L. Maiani, G. Parisi, and R. Petronzio, Nucl. Phys. B **158** (1979) 295.
- [20] D. J. E. Callaway, Phys. Rep. **167** (1988) 241.
- [21] D. J. E. Callaway and R. Petronzio, Nucl. Phys. B **240** [FS12] (1984) 577.
- [22] J. L. Cardy, in *Finite-Size Scaling*, edited by J. L. Cardy, page 1, North-Holland, Amsterdam, 1988.
- [23] A. Coniglio and W. Klein, J. Phys. A **13** (1980) 2775.
- [24] M. Creutz, *Quarks, Gluons and Lattices*, Cambridge Univ. Press, 1983.
- [25] M. Creutz, *Quantum Fields on the Computer*, World Scientific, Singapore, 1992.

- [26] R. Dashen and H. Neuberger, *Phys. Rev. Lett.* **50** (1983) 1897.
- [27] A. K. De and J. Jersák, Yukawa models on the lattice, in *Heavy Flavours*, edited by A. J. Buras and M. Lindner, page 732, World Scientific, Singapore, 1993.
- [28] C. A. de Carvalho, S. Caracciolo, and J. Fröhlich, *Nucl. Phys. B* **215** [FS7] (1983) 209.
- [29] T. A. DeGrand, The present and future of lattice qcd, in *Computational Methods in Field Theory Lecture Notes in Physics 409*, edited by H. Gausterer and C. B. Lang, page 159, Springer-Verlag, Berlin, Heidelberg, 1992.
- [30] M. Falcioni, E. Marinari, M. L. Paciello, G. Parisi, and B. Taglienti, *Phys. Lett. B* **108** (1982) 331.
- [31] A. M. Ferrenberg and R. H. Swendsen, *Phys. Rev. Lett.* **61** (1988) 2635.
- [32] A. M. Ferrenberg and R. H. Swendsen, *Computers in Physics* **Sept./Oct.** (1989) 101.
- [33] A. M. Ferrenberg and R. H. Swendsen, *Phys. Rev. Lett.* **63** (1989) 1195.
- [34] H. R. Fiebig and R. M. Woloshyn, *Nucl. Phys. B (Proc. Suppl.)* **30** (1993) 883.
- [35] H. R. Fiebig, R. M. Woloshyn, and A. Dominguez, Meson-meson scattering phase shifts in 2+1 dimensional lattice qed, preprint FIU-PHY-92-10-23, 1992.
- [36] M. E. Fisher, in *Lectures in Theoretical Physics*, edited by W. E. Brittin, volume VIIC, page 1, Gordon and Breach, New York, 1968.
- [37] M. E. Fisher, in *Critical Phenomena, Proc. of the 51th Enrico Fermi Summer School, Varena*, edited by M. S. Green, Academic Press, New York, 1972.
- [38] M. E. Fisher and M. Randeria, *Phys. Rev. Lett.* **56** (1986) 2332.
- [39] C. Frick et al., *Nucl. Phys. B* **331** (1990) 515.
- [40] J. Fröhlich, *Nucl. Phys. B* **200** [FS5] (1982) 281.
- [41] J. Gasser and H. Leutwyler, *Ann. Phys.* **158** (1984) 142.
- [42] J. Gasser and H. Leutwyler, *Phys. Lett. B* **184** (1987) 83.
- [43] J. Gasser and H. Leutwyler, *Nucl. Phys. B* **307** (1988) 763.
- [44] C. R. Gatttringer, I. Hip, and C. B. Lang, *Nucl. Phys. B (Proc. Suppl.)* **20** (1993) 875.
- [45] C. R. Gatttringer and C. B. Lang, *Phys. Lett. B* **274** (1992) 95.

- [46] C. R. Gatttringer and C. B. Lang, Nucl. Phys. B **391** (1993) 463.
- [47] H. Gausterer and C. B. Lang, Phys. Lett. B **186** (1987) 103.
- [48] K. Gawedzki and A. Kupiainen, Phys. Rev. Lett. **54** (1985) 92.
- [49] J. Glimm and A. Jaffe, Ann. Inst. H. Poincaré **A22** (1975) 13.
- [50] J. Glimm and A. Jaffe, Fortschr. Phys. **21** (1976) 327.
- [51] J. Glimm and A. Jaffe, *Quantum Physics. A Functional Integral Point of View. 2nd Edition*, Springer-Verlag, New York, 1987.
- [52] M. Göckeler, Nucl. Phys. B (Proc. Suppl.) **17** (1990) 347.
- [53] M. Göckeler, H. Kastrup, T. Neuhaus, and F. Zimmermann, Nucl. Phys. B (Proc. Suppl.) **26** (1992) 516.
- [54] M. Göckeler, H. A. Kastrup, T. Neuhaus, and F. Zimmermann, Nucl. Phys. B **404** (1993) 517.
- [55] M. Göckeler and H. Leutwyler, Nucl. Phys. B **350** (1991) 228.
- [56] R. B. Griffiths and P. A. Pearce, Phys. Rev. Lett. **41** (1978) 917.
- [57] R. B. Griffiths and P. A. Pearce, J. Stat. Phys. **20** (1979) 499.
- [58] R. Gupta and A. Patel, Phys. Lett. B **183** (1987) 193.
- [59] T. Hara, J. Stat. Phys. **47** (1987) 57.
- [60] T. Hara and H. Tasaki, J. Stat. Phys. **47** (1987) 99.
- [61] A. Hasenfratz and P. Hasenfratz, Phys. Lett. B **93** (1980) 165.
- [62] A. Hasenfratz and P. Hasenfratz, Nucl. Phys. B **270** [FS16] (1986) 687.
- [63] A. Hasenfratz, P. Hasenfratz, U. Heller, and F. Karsch, Phys. Lett. B **140** (1984) 76.
- [64] A. Hasenfratz et al., Nucl. Phys. B **356** (1991) 332.
- [65] A. Hasenfratz, K. Jansen, C. B. Lang, T. Neuhaus, and H. Yoneyama, Phys. Lett. B **199** (1987) 531.
- [66] P. Hasenfratz, Nucl. Phys. B (Proc. Suppl.) **9** (1989) 3.
- [67] P. Hasenfratz and H. Leutwyler, Nucl. Phys. B **343** (1990) 241.
- [68] P. Hasenfratz and J. Nager, Z. Physik C **37** (1988) 477.
- [69] P. Hasenfratz and F. Niedermayer, Perfect lattice action for asymptotically free theories, preprint BUTP-93/17, 1993.

- [70] U. M. Heller, Nucl. Phys. B (Proc. Suppl.) **17** (1990) 649.
- [71] U. M. Heller, Status of the higgs mass bound, preprint FSU-SCRI-93-144, talk presented at LATTICE 93 in Dallas, 1993.
- [72] U. M. Heller, M. Klomfass, H. Neuberger, and P. Vranas, Nucl. Phys. B (Proc. Suppl.) **26** (1992) 522.
- [73] U. M. Heller, M. Klomfass, H. Neuberger, and P. Vranas, Nucl. Phys. B **405** (1993) 555.
- [74] U. M. Heller, H. Neuberger, and P. Vranas, Phys. Lett. B **283** (1992) 335.
- [75] J. E. Hirsch and S. H. Shenker, Phys. Rev. B **27** (1983) 1736.
- [76] B. Hu, Phys. Rep. **91C** (1982) 233.
- [77] C. Itzykson and J.-M. Drouffe, *Statistical Field Theory*, Cambridge University Press, Cambridge, 1989.
- [78] K. Jansen, J. Kuti, and C. Liu, Phys. Lett. B **309** (1993) 119.
- [79] K. Jansen, J. Kuti, and C. Liu, Nucl. Phys. B (Proc. Suppl.) **30** (1993) 681.
- [80] K. Jansen and C. B. Lang, Phys. Rev. Lett. **66** (1991) 3008.
- [81] P. W. Kasteleyn and C. M. Fortuin, J. Phys. Soc. Jpn. (Suppl.) **26** (1969) 11.
- [82] P. W. Kasteleyn and C. M. Fortuin, Physica (Utrecht) **57** (1972) 536.
- [83] R. Kenna, Finite-size scaling in the $O(N)$ ϕ_4^4 model, hep-lat/9307003, 1993.
- [84] R. Kenna and C. B. Lang, Phys. Lett. B **264** (1991) 396.
- [85] R. Kenna and C. B. Lang, Nucl. Phys. B (Proc. Suppl.) **30** (1993) 697.
- [86] R. Kenna and C. B. Lang, Nucl. Phys. B **393** (1993) 461.
- [87] J. Kuti, L. Lin, and Y. Shen, Nucl. Phys. B (Proc. Suppl.) **4** (1988) 397.
- [88] J. Kuti, L. Lin, and Y. Shen, Phys. Rev. Lett. **61** (1988) 678.
- [89] C. B. Lang, Phys. Lett. B **155** (1985) 399.
- [90] C. B. Lang, Nucl. Phys. B **265** [FS15] (1986) 630.
- [91] C. B. Lang, Phys. Lett. B **229** (1989) 97.
- [92] C. B. Lang and M. Salmhofer, Phys. Lett. B **205** (1988) 329.
- [93] C. B. Lang and U. Winkler, Phys. Rev. D **47** (1993) 4705.
- [94] I.-H. Lee, Nucl. Phys. B (Proc. Suppl.) **4** (1988) 373.

- [95] H. Leutwyler, Phys. Lett. B **189** (1987) 197.
- [96] M. Lüscher, Commun. Math. Phys. **105** (1986) 153.
- [97] M. Lüscher, in *Fields, Strings and Critical Phenomena, Les Houches, Session XLIX, 1988*, edited by E. Brézin and J. Zinn-Justin, Elsevier, Amsterdam, 1989.
- [98] M. Lüscher, Nucl. Phys. B **364** (1991) 237.
- [99] M. Lüscher, Nucl. Phys. B **354** (1991) 531.
- [100] M. Lüscher and P. Weisz, Nucl. Phys. B **290** [FS20] (1987) 25.
- [101] M. Lüscher and P. Weisz, Nucl. Phys. B **295** [FS21] (1988) 65.
- [102] M. Lüscher and P. Weisz, Nucl. Phys. B **318** (1989) 705.
- [103] M. Lüscher and U. Wolff, Nucl. Phys. B **339** (1990) 222.
- [104] S.-K. Ma, *Modern Theory of Critical Phenomena*, Benjamin/Cummings Publ. Co. Inc., Reading, MA, 1976.
- [105] S.-K. Ma, Phys. Rev. Lett. **37** (1976) 461.
- [106] F. Martinelli and E. Olivieri, Some remarks on pathologies of renormalization-group transformations for the ising-model, Univ. Roma preprint, 1993.
- [107] N. Metropolis, A. W. Rosenbluth, A. H. Teller, and E. Teller, J. Chem. Phys. **21** (1953) 1087.
- [108] I. Montvay and P. Weisz, Nucl. Phys. B **290** [FS20] (1987) 327.
- [109] G. Murthy and R. Shankar, Phys. Rev. B **32** (1985) 5851.
- [110] H. Neuberger, Phys. Lett. B **199** (1987) 536.
- [111] H. Neuberger, Phys. Rev. Lett. **60** (1988) 889.
- [112] H. Neuberger, Nucl. Phys. B (Proc. Suppl.) **17** (1990) 17.
- [113] T. Neuhaus, Nucl. Phys. B (Proc. Suppl.) **9** (1989) 21.
- [114] J. Nishimura, Phys. Lett. B **294** (1992) 375.
- [115] K. Osterwalder and E. Seiler, Ann. Phys. **110** (1978) 440.
- [116] C. Rebbi, *Lattice Gauge Theories and Monte Carlo Simulations*, World Scientific, Singapore, 1983.
- [117] G. Roepstorff, *Pfadintegrale in der Quantenphysik*, Vieweg: Braunschweig, 1991.

- [118] H. J. Rothe, *Lattice Gauge Theories - An Introduction*, World Scientific, Singapore, 1992.
- [119] M. Sato, T. Miwa, and M. Jimbo, Proc. Japan Acad. , Ser. A **53** (1977) 6.
- [120] E. Seiler, *Gauge Theories as a Problem of Constructive Quantum Field Theory and Statistical Mechanics*, Springer Lecture Notes in Physics 159, Springer, Berlin, 1982.
- [121] R. Shankar, R. Gupta, and G. Murthy, Phys. Rev. Lett. **55** (1985) 1812.
- [122] S. H. Shenker and J. Tobochnik, Phys. Rev. B **22** (1980) 4462.
- [123] A. Sokal, Monte carlo methods in statistical physics: Foundations and new algorithms, Lecture Notes Cours de Troisieme Cycle de la Physique en Suisse Romande, Lausanne, 1989.
- [124] A. Sokal, Nucl. Phys. B (Proc. Suppl.) **20** (1991) 55.
- [125] H. Stanley, *Introduction to Phase Transitions and Critical Phenomena*, Oxford University Press, New York, 1971.
- [126] D. Stauffer, Phys. Rep. **54** (1979) 1.
- [127] M. Sweeny, Phys. Rev. B **27** (1983) 4445.
- [128] R. H. Swendsen, Phys. Rev. Lett. **42** (1979) 859.
- [129] R. H. Swendsen, Phys. Rev. Lett. **52** (1984) 1165.
- [130] R. H. Swendsen, Phys. Rev. Lett. **52** (1984) 2321.
- [131] R. H. Swendsen and J.-S. Wang, Phys. Rev. Lett. **58** (1987) 86.
- [132] K. Symanzik, J. Math. Phys. **7** (1966) 510.
- [133] K. Symanzik, in *Proc. Int. School of Physics "Enrico Fermi", Varenna Course XLV*, edited by R. Jost, Academic Press, 1969.
- [134] K. Symanzik, Nucl. Phys. B **226** (1983) 187.
- [135] M. M. Tsypin, The effective potential of the lattice ϕ^4 theory and the upper bound on the higgs mass, Lebedev Phys. Inst. Moscow preprint 280, 1985.
- [136] A. C. D. van Enter, R. Fernández, and A. D. Sokal, Phys. Rev. Lett. **66** (1991) 3253.
- [137] A. C. D. van Enter, R. Fernández, and A. D. Sokal, to appear in: J. Stat. Phys (1993).
- [138] J.-S. Wang and D. Stauffer, Z. Phys. B **78** (1990) 145.

- [139] J. Westphalen, F. Zimmermann, M. Göckeler, and H. A. Kastrup, Scattering phases in the broken phase of the 4-d $o(4)$ non-linear σ -model, Contrib. to LATTICE 93 in Dallas, 1993.
- [140] C. Whitner, PhD Thesis, Princeton University, 1984.
- [141] K. G. Wilson, Phys. Rev. B **4** (1971) 3184.
- [142] K. G. Wilson, Phys. Rev. D **10** (1974) 2445.
- [143] K. G. Wilson and J. Kogut, Phys. Rep. **12C** (1974) 76.
- [144] U. Wolff, Phys. Rev. Lett. **62** (1989) 361.
- [145] U. Wolff, High precision simulations with fast algorithms, in *Computational Methods in Field Theory, Lecture Notes in Physics 409*, edited by H. Gausterer and C. B. Lang, page 127, Springer-Verlag, Berlin, Heidelberg, 1992.
- [146] C. N. Yang and T. D. Lee, Phys. Rev. **87** (1952) 404.
- [147] C. N. Yang and T. D. Lee, Phys. Rev. **87** (1952) 410.
- [148] F. Zimmermann, Unstable particles in finite volume: the broken phase of the 4-d $o(4)$ non-linear σ -model, RHTH Aachen PhD Thesis, 1993.
- [149] F. Zimmermann, J. Westphalen, M. Göckeler, and H. A. Kastrup, Nucl. Phys. B (Proc. Suppl.) **30** (1993) 879.